

NASA Contractor Report 187221

IN-32
77720
P-59

Optical Multiple Access Techniques for On-Board Routing

Antonio J. Mendez and Eugene Park
Mendez R&D Associates
El Segundo, California

and

Robert M. Gagliardi
University of Southern California
Los Angeles, California

March 1992

Prepared for
Lewis Research Center
Under Contract NAS3-25925

NASA
National Aeronautics and
Space Administration

(NASA-CR-187221) OPTICAL MULTIPLE ACCESS
TECHNIQUES FOR ON-BOARD ROUTING Final Report
(Mendez R and D Associates) 59 p CSCL 17B

N92-25432

Unclas
G3/32 007720



NASA LeRC NAS3-25925 Final Report

Table of Contents

	PAGE
Foreword	ii
1.0 Introduction and Summary	1-1
2.0 Requirements Analysis	2-1
3.0 Conceptual Design of Three Candidate Photonic Networks ..	3-1
4.0 Analysis and Trade Offs of The Three Candidates	4-1
5.0 Selection of Preferred Candidate for Phase II and Refinement of Its Specifications	5-1
6.0 Bill of Materials for Preferred Candidate	6-1
7.0 Bit Error Rate Analysis of Preferred Candidate and Applicable Error Correction Codes and Alternatives	7-1
8.0 Demonstration and Evaluation of Subscale Temporal and Temporal/Spatial CDMA Networks	8-1
9.0 Identification of System/Technology Shortfalls and Future R / R&D Recommendations	9-1
10.0 Conclusions and Phase II Recommendations	10-1
11.0 References	11-1

Foreword

This is the Final Report on SBIR Phase I Contract NAS3-25925 between NASA LeRC and Mendez R&D Associates. The NASA LeRC Project Manager was William D. Ivancic, Digital Systems Technology Branch. The Principal Investigator was Antonio J. Mendez. He was supported by Eugene Park (optical communications engineer) and Prof. Robert M. Gagliardi (University of Southern California, Consultant). We would like to acknowledge helpful discussions and computations provided by Mark Dale (TRW and USC) and also the support of Bradley D. Sherman (Douglas Aircraft Company) in testing the subscale breadboard. Sonjia Fielder (Hughes Aircraft Company and USC) was very effective in compiling the vendor survey on candidate laser transmitters and receivers for the various optical multiple access networks considered on this program.

1.0 Introduction and Summary

"Design and analyze an optical multiple access system, based on Code Division Multiple Access (CDMA) techniques, for on board crosslink applications on a future communication satellite. The CDMA system shall serve eight (8) concurrent users at a point to point (port to port) data rate of 180 Mb/s. (At the start of this program the bit error rate requirement (BER) was undefined, so it was treated as a design variable during the contract effort.)

Temporal, temporal/spatial hybrids, and single pulse per row (SPR, sometimes termed "sonar matrices") types of CDMA designs shall be considered and traded off. One preferred design approach shall be selected. The Phase I effort shall culminate with a specific design and component selection for feasibility demonstration in a follow-on phase."

The description summarized above is consistent with the proposal and the Program Overview which was presented at the Kickoff Meeting.

The optical multiple access system is to effect the functions of a circuit switch under the control an autonomous network controller as shown in Figure 1-1. The generic optical multiple access system which can support temporal, temporal/spatial, or single pulse per row (SPR) CDMA techniques is shown in Figure 1-2.

We have carried out the design, analysis, and trade offs required by the statement of work and have selected a temporal/spatial CDMA scheme which has SPR properties. This selected design can be implemented with off the shelf components (which are identified in the bill of materials). The selected design will meet the system specifications as stated here. The complete photonic network architecture of the selected design is shown in Figure 1-3 and the specific matrix codes $M(8,4,4)$ are shown in Figure 1-4. The network requires eight laser transmitters with laser pulses of 0.93 ns operating at 180 Mb/s and 8-13 dBm peak power. It requires 8 PIN diode receivers with sensitivity of -27 dBm for 0.93 ns pulses.

Bit error rate (BER) computations, based on both electronic noise and intercode crosstalk, were estimated for the selected design. The raw BER (10^{-3}) performance when all eight users are communicating concurrently is moderately acceptable. If better BER performance is required, then we show how this can be obtained with error correction codes (ECC) using near term electronic technology.

If ECC, for example Reed-Solomon (54, 38, 8) encoding is selected, then the laser transmitter would operate at 256 Mb/s with pulses of 0.65 ns. Alternatively, a higher weight matrix CDMA code which need not rely on ECC can be used (at the expense of higher risk optical technologies). The BER for this alternate case was computed and found to be quite good (10^{-7} - 10^{-9})

A subscale CDMA network which was built with resources outside of this contract was used to demonstrate and evaluate the concepts developed in this program. The test results support and validate the analyses and claims made for the selected design.

We reviewed the function flow and all interfaces involved in the optical multiple access system crosslink. We have identified technology shortfalls. Most of these are of systems technology type or require the refocussing of ongoing device technology. Major breakthroughs are not required in order to make the CDMA network realizable.

Six areas that merit additional R / R&D are: (1) further development of matrix codes, especially T/S -SPR combinations; (2) reconfigurable matrix encoders or decoders; (3) zero loss CDMA photonic networks (this would allow a larger selection of communications transceivers, more users, or higher data rates); (4) criteria and techniques for establishing receiver thresholds in dynamic, asynchronous multi user environments; (5) error correction codes applicable to optical multiple access networks operating at greater than 200 Mb/s, and (6) system checkout, calibration, and alignment procedures. The material presented in this Introduction and Summary is supported and expanded in the following chapters.

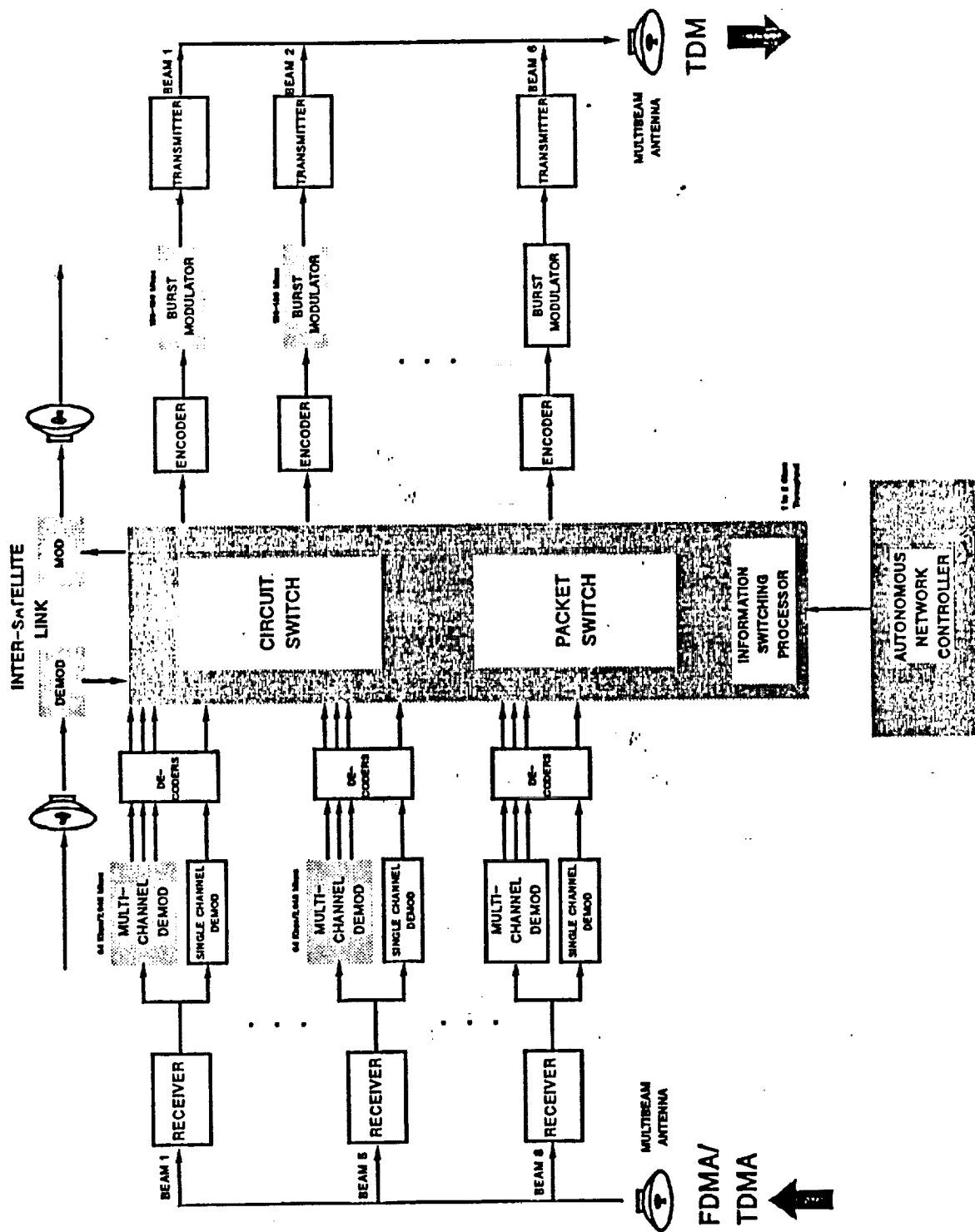


Figure 1-1. Processing Satellite.

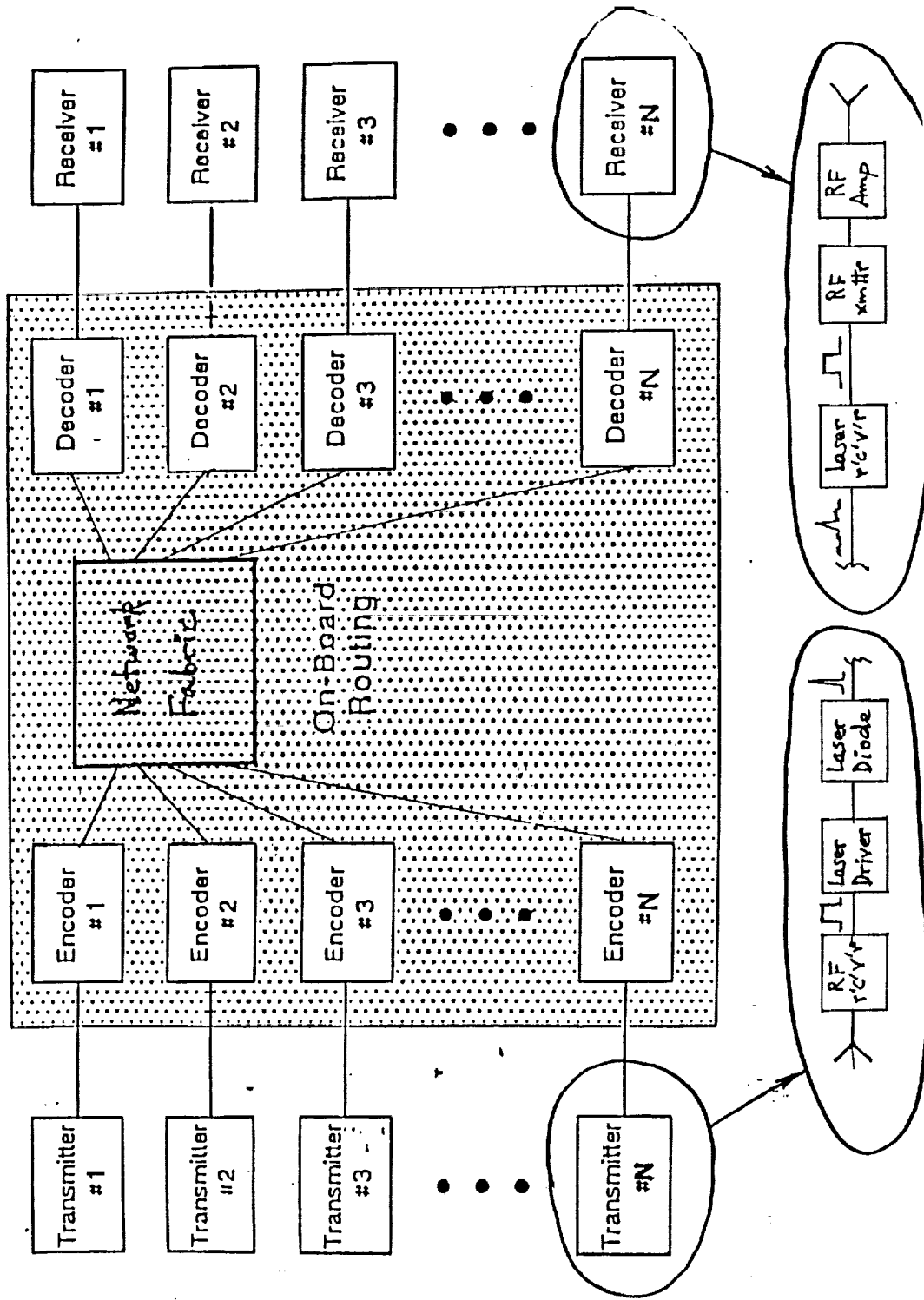


Figure 1-2. Generic Optical Multiple Access System.

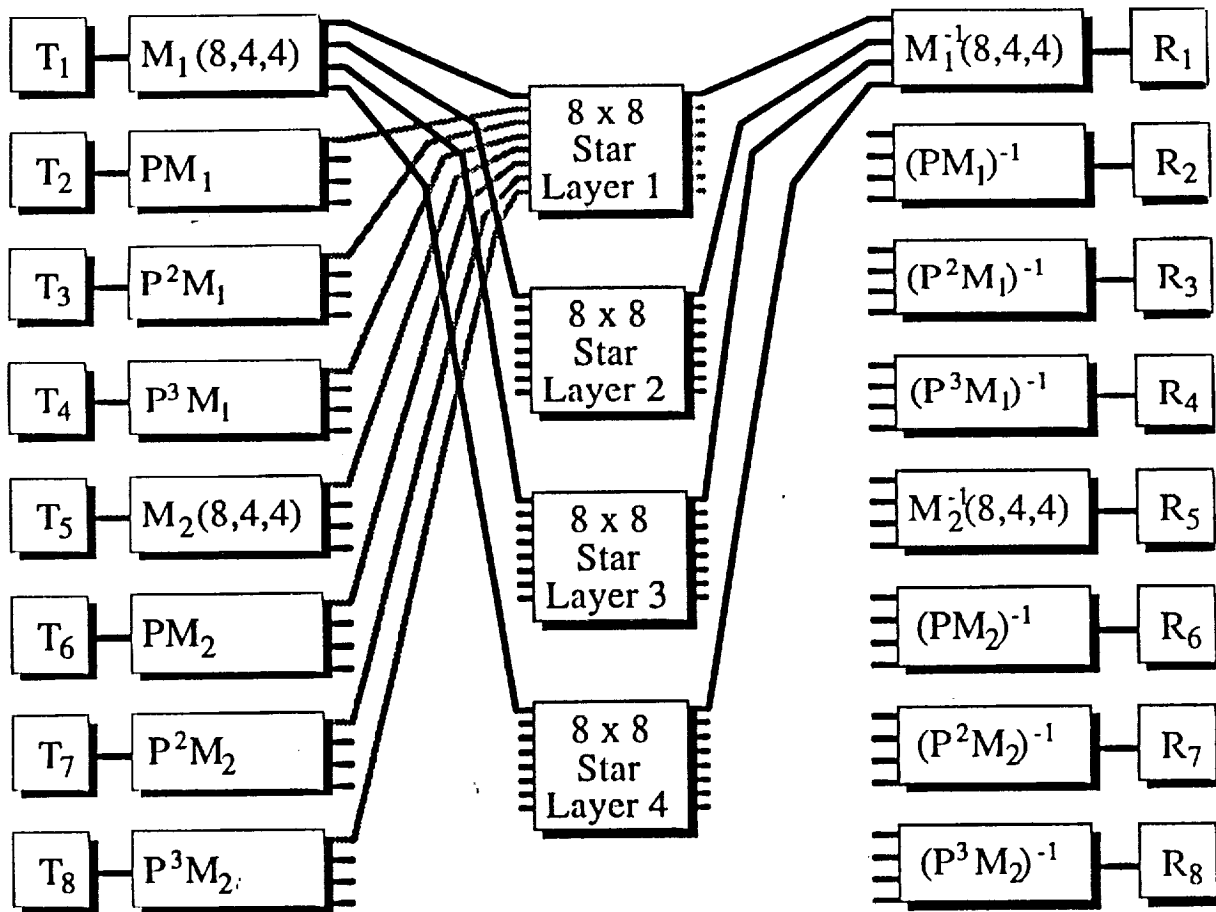
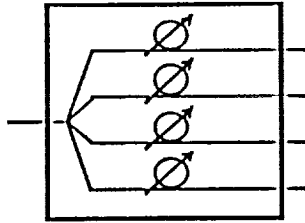


Figure 1-3.

Architecture of Preferred Candidate Photonic Network

- | | |
|------------------|---|
| $M_i(N,w,f)$ | = matrix code i |
| $P^n M_i$ | = n^{th} permutation of matrix M_i |
| M_i^{-1} | = inverse of matrix code i ("optical correlator") |
| $(P^n M_i)^{-1}$ | = inverse of matrix code $P^n M_i$ |
| T_j | = transmitter j |
| R_k | = receiver k |

6/20/91



CODE #1

$$\begin{bmatrix} 1 & 0 & 0 & 0 & 0 & 0 \\ 0 & 1 & 0 & 0 & 0 & 0 \\ 1 & 0 & 0 & 0 & 0 & 0 \\ 0 & 0 & 0 & 1 & 0 & 0 \end{bmatrix}$$

CODE #5

$$\begin{bmatrix} 1 & 0 & 0 & 0 & 0 & 0 \\ 1 & 0 & 0 & 0 & 0 & 0 \\ 0 & 0 & 0 & 0 & 1 & 0 \\ 0 & 1 & 0 & 0 & 0 & 0 \end{bmatrix}$$

CODE #2

$$\begin{bmatrix} 0 & 0 & 0 & 0 & 1 & 0 \\ 1 & 0 & 0 & 0 & 0 & 0 \\ 0 & 1 & 0 & 0 & 0 & 0 \\ 1 & 0 & 0 & 0 & 0 & 0 \end{bmatrix}$$

CODE #6

$$\begin{bmatrix} 0 & 0 & 1 & 0 & 0 & 0 \\ 1 & 0 & 0 & 0 & 0 & 0 \\ 1 & 0 & 0 & 0 & 0 & 0 \\ 0 & 0 & 0 & 0 & 1 & 0 \end{bmatrix}$$

CODE #3

$$\begin{bmatrix} 0 & 1 & 0 & 0 & 0 & 0 \\ 0 & 0 & 0 & 0 & 1 & 0 \\ 1 & 0 & 0 & 0 & 0 & 0 \\ 0 & 1 & 0 & 0 & 0 & 0 \end{bmatrix}$$

CODE #7

$$\begin{bmatrix} 0 & 0 & 0 & 0 & 0 & 1 \\ 0 & 0 & 1 & 0 & 0 & 0 \\ 1 & 0 & 0 & 0 & 0 & 0 \\ 1 & 0 & 0 & 0 & 0 & 0 \end{bmatrix}$$

CODE #4

$$\begin{bmatrix} 0 & 0 & 1 & 0 & 0 & 0 \\ 0 & 1 & 0 & 0 & 0 & 0 \\ 0 & 0 & 0 & 0 & 1 & 0 \\ 1 & 0 & 0 & 0 & 0 & 0 \end{bmatrix}$$

CODE #8

$$\begin{bmatrix} 0 & 1 & 0 & 0 & 0 & 0 \\ 0 & 0 & 0 & 0 & 0 & 1 \\ 0 & 0 & 1 & 0 & 0 & 0 \\ 1 & 0 & 0 & 0 & 0 & 0 \end{bmatrix}$$

Figure 1-4. CDMA Matrix Codes and Their Fiber Optic Implementation.

2.0 Requirements Analysis

The objective of this contract is to identify a viable optical multiple access technique to effect satellite on board routing. The key requirements which drive the selection are, primarily, number of on board users, point to point data rate, and number of concurrent users and, secondarily, transmission bit error rate.

At the kickoff meeting we determined that the number of users was 8 and the point to point data rate was 180 Mb/s, corresponding to the perceived requirements for an Advanced Processing Satellite as shown in Figure 1-1. The bit error rate requirement was unspecified, so we treated it as a design variable.

Many optical multiple access approaches are available [1]. We elected to concentrate on code division multiple access (CDMA) techniques because they lend themselves to asynchronous, bursty, concurrent communications [2,3,4,5]. Also, with some very new developments [6,7,8], CDMA could potentially be implemented with non critical components which could be used in extended, unattended operations such as required by satellite operations.

Three types of optical CDMA are being actively pursued: spectral [5], temporal [3], and temporal/spatial [6,7]. Temporal and temporal/spatial were investigated on this contract because they not only meet the criterion of unattended operation but potentially could be implemented with low cost non critical components.

Temporal CDMA is represented by a code length. The code contains a fixed number ("weight") of pulses called the pulse sequence. The various pulse sequences in the set are pseudo orthogonal to each other so that a receiver, matched to one of the codes, can discriminate between it and the unmatched codes. The matched code produces the autocorrelation. The unmatched codes produce crosscorrelations. The number of pseudo orthogonal codes corresponds to the number of users in the network (e.g., the number of users in the onboard routing switch.) The random, concurrent crosscorrelations give rise to the clutter which must be overcome by an addressed receiver.

Temporal/spatial CDMA is represented by a matrix. The number of columns corresponds to the code length in the time domain. The number of rows corresponds to the number of space-like channels.

Temporal CDMA codes and code lengths can be derived by well defined constructions and algorithms [4]. Temporal/spatial CDMA matrices can be derived from temporal CDMA codes by recently developed design rules [6,7] or by heuristic rules based on sonar matrices [8].

CDMA codes, the number of users in a CDMA network, and the data rate in the network are related by a figure called the chip time (T_c). The chip time is the pulse width of one of the pulses in the CDMA pulse signature.

In the case of temporal CDMA, the chip time is given by

$$T_c(L) = (\text{data rate})^{-1} / L(N,w) \quad (2-1)$$

where $L(N,w)$ is the code length, N the number of users, and w the weight of the code (number of pulses in the code signature).

In the case of temporal/spatial CDMA, the codes are represented by pseudo orthogonal matrices $M(N,w,f)$, where N is the number of users, w the code weight (non null matrix elements) and f is the number of rows in the matrix (also the number of space channels or fibers; hence "f"). The number of columns in the matrix, $L_t(N,w,f)$, is the code length in the time domain. Thus, matrix chip time are related to the matrix codes and data rate by

$$T_c(M) = (\text{data rate})^{-1} / L_t(N,w,f) \quad (2-2)$$

Clearly, $T_c(M) < T_c(L)$. We have searched for solutions of Equations 2-1 and 2-2 for $N \geq 8$, $w \geq 4$, $f \geq 2$ and data rate 180 Mb/s. These requirements were set in order to meet the user and data rate requirements and in order to minimize the multi user interference (MUI) due to concurrent communication in the postulated application.

The three kinds of optical CDMA solutions which we looked for are depicted in Figure 2-1. The candidate 23 initial candidate solutions which emerged from this search are shown in Table 2-1.

In order to reduce these initial 23 candidate solutions to three we required (1) that the laser transmitter not be large, exotic, critical, environmentally sensitive, not in production, or expensive (this leaves out solutions with $T_c \leq 0.40\text{ns}$, therefore all temporal CDMA) and (2) all matrix CDMA with $T_c \leq 0.40\text{ns}$ and/or $f = \text{odd number}$ (except $f=7$). This is because $f = \text{odd}$ leads to odd number splitters and combiners in the associated network fabric, and these are generally unavailable or custom items or have limited growth potential for other applications.

This initial screening gives three matrix candidates meriting further analysis:

- (1) M(8,4,4)
- (2) M(12,4,4)
- (3) M(16,4,7)

and an alternate

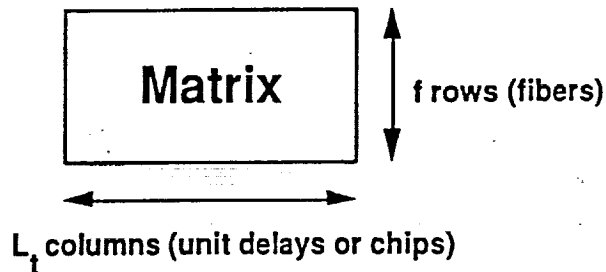
- (1') M(8,8,4)

All of these meet the user and data rate requirements. These are analyzed and traded off in the next chapter in order to produce a preferred selection.

Figure 2-1.

Types of CDMA Codes Considered

- Linear CDMA $L(N,w)$ $N \geq 8$, $w = \text{variable}$
then chip time = $T_c = (\text{data rate})^{-1} / L(N,w)$
- Matrix CDMA $M(N,w,f)$ $N \geq 8$, w and $f = \text{variable}$



then chip time = $T_c = (\text{data rate})^{-1} / L_t(N,w,f)$.

Matrices were of two kinds: (1) Temporal/spatial (T/S) derived from $L(N,w)$ and (2) Single pulse per row (SPR) derived from Sonar matrices

- Data rate in all cases was 180 Mb/s.

06-21-91

Table 2-1. Optical CDMA Candidate Solutions.

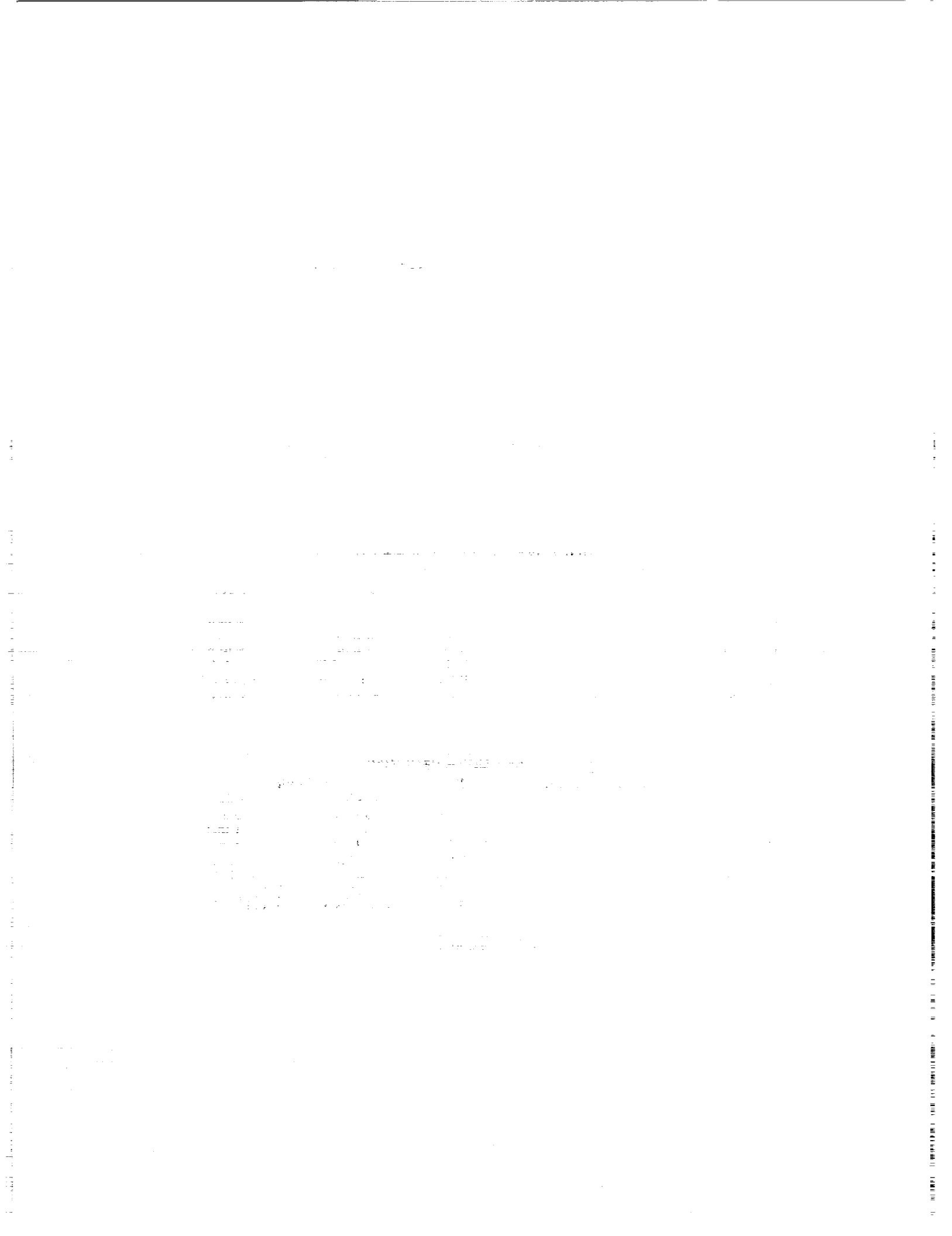
Table 1. Temporal CDMA Parameters*			
Users, N	Weight, w	Chip Time, T _c (ps)	Peak Power, P(dBm)
8	4	113	12-17
8	5	69	16-21
8	6	46	19-24
8	8	23	24-29
8	10	14	28-33
12	4	76	14-19
12	5	46	18-23
16	4	57	15-20
16	5	35	19-24

* an APD receiver with -30dBm sensitivity was assumed

Temporal/Spatial Hybrid CDMA Parameters						
N	w	Space channels, f	T _c (ns)	APD**	P(dBm)	PIN***
8	4	4	1.11	-5 to 0		0 to 5
8	4 (SPR)	4	0.93	-5 to 0		0 to 5
8	4	2	0.40	-8 to -3		-3 to 2
8	10	4	0.20	-1 to 4		4 to 9
12	4	2	0.29	-6.2 to -1.2		-1.2 to 3.8
12	4	4	0.93	-3.2 to 1.8		1.8 to 6.8
16	4	4	0.69	-2 to 3		3 to 8

Table 2. SPR CDMA Parameters						
N	w	Space channels, f	T _c (ns)	APD**	P(dBm)	PIN***
8	4	4	0.93	-5 to 0		0 to 5
8	4 (T/S)	5	1.39	-4 to -1		1 to 4
8	4	5	1.85	-4 to -1		1 to 4
12	4	6	1.39	-1.4 to 3.6		3.6 to 8.6
12	4	6	1.85	-1.4 to 3.6		3.6 to 8.6
16	4	7	1.39	0.4 to 5.4		5.4 to 10.4
16	4	7	1.85	0.4 to 5.4		5.4 to 10.4

** at -40 dBm
 *** at -35 dBm



3.0 Conceptual Design of Three Candidate Photonic Networks

The three candidates photonic network identified in Chapter 2.0 all are variants of the type same temporal/ spatial CDMA network shown in Figure 3-1. The encoders/decoders are of the matrix type, all encoders/decoders are derivable by permutation from a few basic matrices which themselves are derivable from linear pseudo orthogonal codes, the network fabric is that of layered stars, the weight of the codes is the same ($w=4$, except for the alternate which has $w=8$), the parallelism is the same ($f=4$ except for the third candidate for which $f=7$), and the pulses per row for all basic matrices and their permutations is the same (pulses/row=1 or 2). This similarity among the three candidate allows us to concentrate on the system requirements (users, 8; data rate, 180Mb/s) while leaving the raw bit error rate, cost, and complexity as derived characteristics for each candidate.

The basic distinctions among these three candidates are:

- (1) M (8,4,4). Most compact, least complex candidate satisfying the user and data rate requirements. Simple, low loss components. Off the shelf passive and active components. May have problems with crosstalk and clutter (at BER requirements better than 10^{-3}), hence needs adaptive threshold and error correction code technologies (see Chapter 7.0). Has M(8,8,4) as alternate.
- (2) M (12,4,4). Intermediate candidate satisfying the user and data rate requirements. Simple, low loss components. Off the shelf passive and active components solves crosstalk/clutter problem by only using 8 of 12 possible codes (which can be preselected for minimum interference). Less reliance on adaptive threshold and error correction codes. Excess network capability can be used for growth potential or for back up in case of failure. No alternative design identified.
- (3) M (16,4,7). High end candidate satisfying the user and data rate requirements. Intermediate, modest loss components. Off the shelf active components, somewhat unique passive components. Higher complexity layering. Solves crosstalk/clutter problem by grossly thinning the number of user codes (8 out of 16, picked for minimum interference). Least reliance on adaptive threshold and error correction codes. Excess network capability can be used for growth potential or for back up in case of failure. No alternative design identified.

In the next chapter the three candidates and their properties will be analyzed and traded off with respect to BER, cost, and complexity.

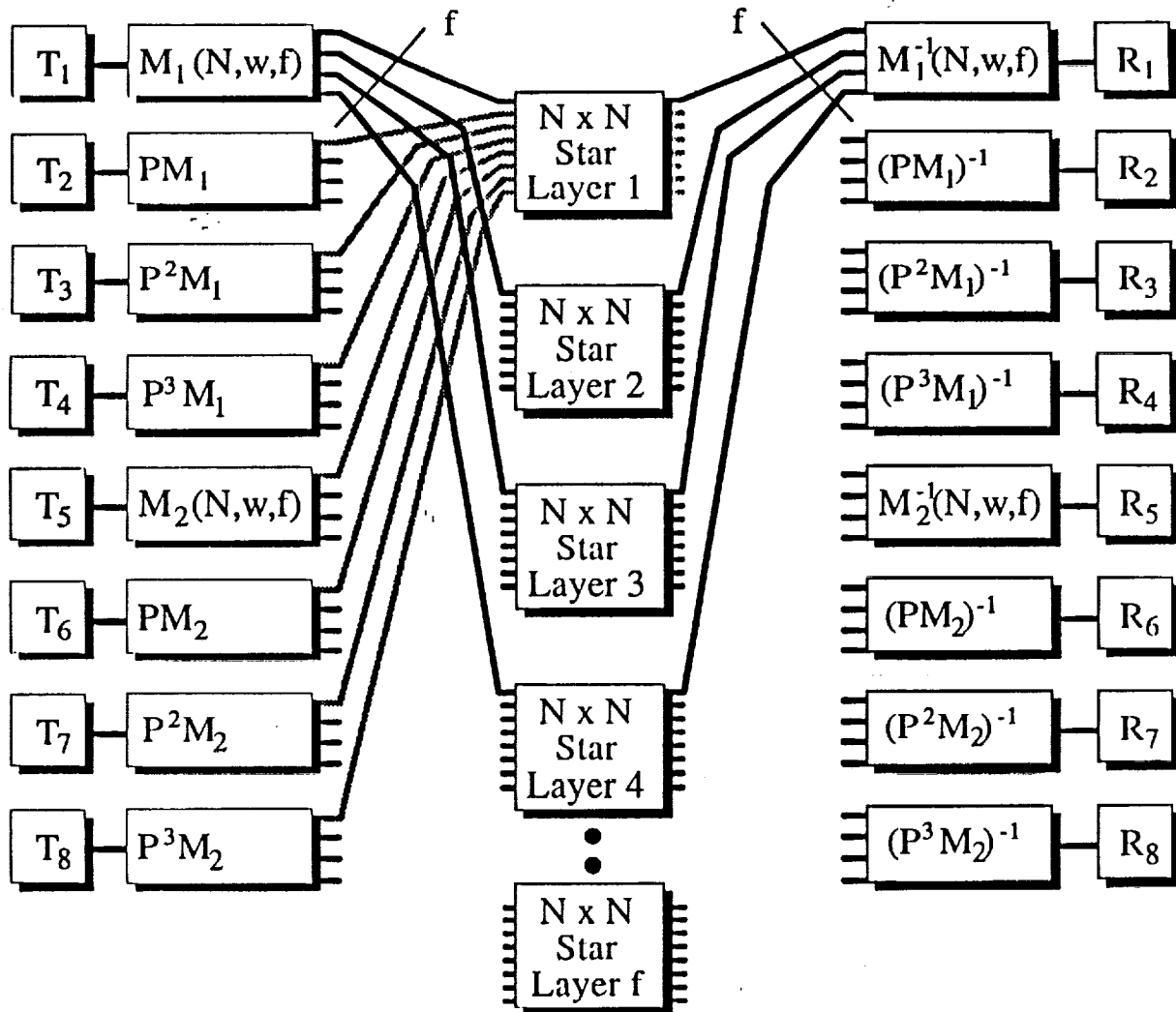


Figure 3-1.

Architecture of Candidate Photonic Networks

- $M_i(N,w,f)$ = matrix code i
- $P^n M_i$ = n^{th} permutation of matrix M_i
- M_i^{-1} = inverse of matrix code i ("optical correlator")
- $(P^n M_i)^{-1}$ = inverse of matrix code $P^n M_i$
- T_j = transmitter j
- R_k = receiver k
- $M(N,w,f)$ = $M(8,4,4), M(12,4,4), M(16,4,7)$

6/21/91

4.0 Analysis and Trade offs of Three Candidates

Since the three candidates satisfy the user and data rate requirements, the important analyses are related to bit error rate (BER) performance and component selection.

Computer Simulation of BER Performance

With respect to BER, the only critical candidate is the M(8,4,4) because the M(12,4,4) and M(16,4,7) candidates operate far from the clutter limited case (at most 8 of 12 or 8 of 16 codes are used at any one time).

During this portion of the program, a computer simulation of the M(8,4,4) CDMA network was generated. The computer simulation modeled the transmitter, encoding, broadcasting, decoding, and receiver functions for all channels. The various transmitters had variable delays among them, representing asynchronicity.

The output of a given receiver was monitored as its matched transmitter sent "1's" or "0's", as a function of the number of asynchronous, concurrent transmitters. 10,000 random code shifts were run on the computer in order to capture the statistics of this process. The output of the receiver when its matched transmitter is sending a "1" is called the signal; when transmitting a "0", it is called the clutter. (the superposition of crosstalk from all concurrent, asynchronous, unmatched transmitters).

Worst case code shifts that maximize the clutter were also computed. The results of this computer simulation are summarized in Figure 4-1. The top graph shows the signal and clutter as a function of the number of users. The graph shows that (1) the average of the signal and clutter are well separated with up to 8 concurrent users, (2) the clutter plus RMS is below the minimum signal, and (3) there is a well defined threshold that separates signal and clutter with up to 4 interfering users (even in the worst case).

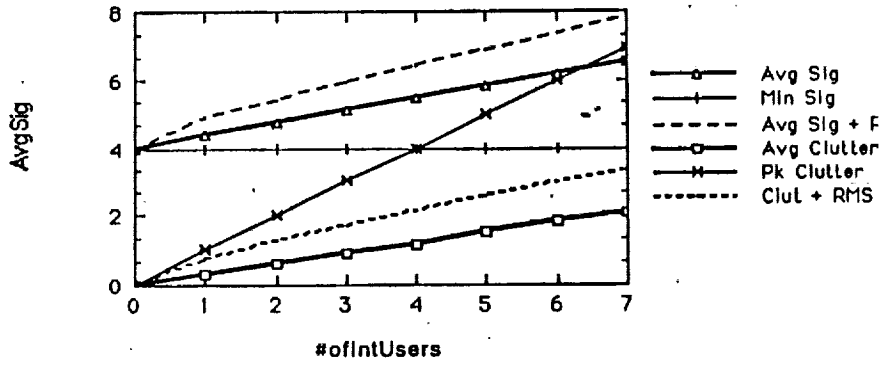
The statistics of the signal and of the clutter for eight concurrent users are shown in the lower two graphs. We can see the separation of the signal and clutter, but with an overlap of the tails of the distributions. This overlap is the source of the BER and, clearly, the receiver threshold must be located in such a way that the drop outs and drop ins are minimized.

A more exact computation of the resulting BER is given in Chapter 7.0. A discussion of the criticality of an adaptive threshold is given there, also.

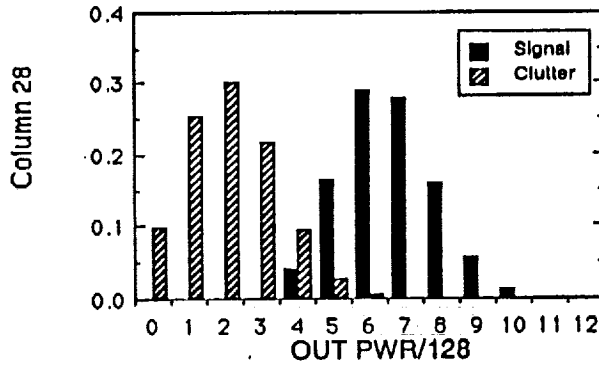
The overlap of signal and clutter distributions can be controlled by increasing the separation of these distributions - by increasing the code weight, for example. That is why the M(8,8,4) is the alternate candidate to the M(8,4,4).

Figure 4-1. Computer Simulation of Mutual Interference.

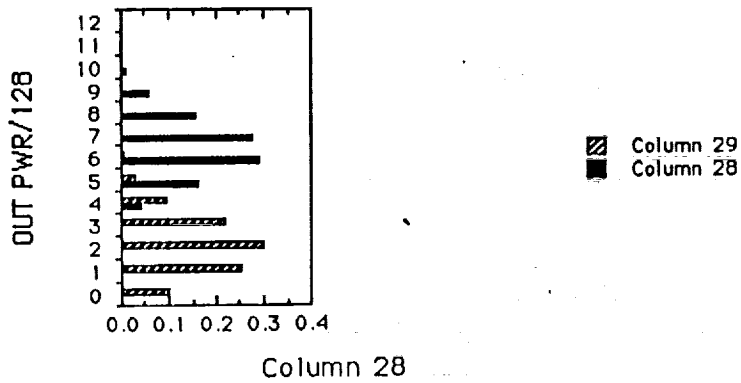
Data from 11_9
 SPR Codes - Output of Dec#1 with 10000 Random Code Shifts of $\pm 5T_c$
 (Interf: #2, #3, #4, #5, #6, #7 #0)



Data from "11_9"
 100 Random Code Shifts



Data from "11_9"



Component Analysis

A vendor survey was carried out in order to determine the availability and cost of the transceivers discussed in Chapter 2.0. We found that, whereas the receiver requirements discussed in 2.0 are theoretically achievable, such receivers are not commercially available. Thus, the receiver sensitivity was reduced by 8 dBm and the transmitter requirements increased by this same amount - to keep the same power budget and to make the components commercially available.

Tables 4-1a (M(8,4,4)), -1b (M(12,4,4)), and -1c (M(16,4,7)) show the results of the vendor survey.

We see that M(8,4,4) can be implemented with transceiver combinations such as

Transmitter:	IPITEK TX-500
Receiver:	Laser Diode LDPM-1000
	or
	BT&D RCV 1201-1.2

These combinations handle the basic M(8,4,4) requirements or the M(8,4,4) with error correction codes. The error correction codes require a larger channel bit data rate as well as a smaller channel bit chip time. Various combinations of transceivers can handle these requirements, so we say that the M(8,4,4) is compatible with ECC.

M(12,4,4) and M(16,4,7) can be implemented with off the shelf transceivers which are compatible with an ECC overlay. (As noted earlier, these two codes are less dependent on ECC because the networks are not fully populated.) These candidates require higher powered laser diode transmitters, so that they will tend to be more expensive and to limit growth potential.

With respect to the passive components, all candidates are based on off the shelf components, but the component cost increases in the order M(8,4,4), M(12,4,4), M(16,4,7).

Growth Potential

This characteristic is a measure of adaptability to other applications which may have requirements for higher data rates users, or both. Also, this characteristic is a measure of whether, in going to these higher requirements, the cost and complexity is severely increased.

Both the M(8,4,4) and M(12,4,4) have growth potential from this viewpoint. The M(16,4,7) encoders, if they are to be reconfigurable, require 1x7 splitters / combiners and seven channel ribbon cable. These have limited commercial availability and this may limit this candidate's growth potential.

Table 4-1a. Transceiver Candidates for M(8,4,4).

TRANSMITTER REQTS		TRANSMITTER CANDIDATES/COST		RECEIVER REQTS		RECEIVER CANDIDATES/COST	
P(dBm)	Tc	S(dBm)	1/c BW	-27. PIN			
8-13	0.93ns						
1. T/S, SPR (8,4,4)							
		1. **MASH-TECH [0-3dBm, 0.80ns] (850nm)	\$800-\$400 per model		1. ANTEL [30dBm]		\$4,500
		2. **BCP [0dBm, 0.75ns] (850nm)	\$3,700		model: MARX-DP		
		3. **OpioElectronics [0dBm, 0.65ns] (1300nm)	\$6,800		model: PAD-110	2. ****OpioElectronics [-23 dBm]	\$1,600
		4. **LaserDiode [0dBm, 0.60ns] (1300nm)	\$2,495		model: DRX-878	3. ****PCO [-29dBm]	\$4,200
		5. Teletronics [14.7dBm, 0.30ns] (1300nm)	\$10,300		4. LaserDiode [-27dBm]	model: DRX-878	
		6. Teletronics [11.7dBm, 0.30ns] (1300nm)	\$10,500		model: LDPM-1000 (at 10^-9 BER)	5. BT & D [-30 dBm]	\$1,000 per
		7. IPITEK [10dBm, 0.40ns] (1300nm)	\$2,700		model: RCV 1201-1.2	6. Teletronics [will see 30ps]	\$1,600 per
		8. SONY [6.99 dBm, 0.50ns] (1300nm)	***		model: SD46, SD30 & CSA803 Mainframe		\$45,525
		9. SONY [13 dBm, 0.50ns]	\$90 per				
		10. SONY [14 dBm, 0.50ns]	\$90 per				
		11. SONY [15 dBm, 0.50ns]	\$190 per				
		12. SONY [20 dBm, 0.50ns]	***				
		13. SONY [17 dBm, 0.50ns]	\$180 for 3				
		14. SONY [20 dBm, 0.50ns]	***				
		15. SONY [23 dBm, 0.50ns]	***				
		16. SONY [26 dBm, 0.50ns]	***				
		17. SONY [30 dBm, 0.50ns]	***				

** Model not able to meet power requirements

*** Not available through distribution

Table 4-1b. Transceiver Candidates for M(12,4,4).

CDMA SYSTEM	TRANSMITTER REQ'TS		RECEIVER REQ'TS		RECEIVER CANDIDATES/COST
	P (dBm)	Tc	S (dBm)	1/τc BW	
2. T/S(12,4,4)	9.8-14.8	0.93ns		-27. PIN	1. ANTEL [-30dBm] \$4,500 model: MARX-DP 2. ****OpioElectronics [-23 dBm] \$2,600 model: PAD-110 \$4,200 3. *****PCO [-29dBm] model: DRX-678 4. LaserDiode [-27dBm] \$1,000 per model: LDPN-1000 (at 10^-9 BER) \$45,525 5. Tektronics [will see 30ps] \$1,600 per model: SD-46, SD30, & CSA803 Mainframe 6. BT & D [-30 dBm] model: RCY 1201-1.2
			1. **MASH-TECH [0-3dBm, 0.80ns] \$800-\$400 per model: (850nm) 2. **BCP [0dBm, 0.75ns] \$3,700 model: 400 (850nm) 3. **OpioElectronics [0dBm, 0.65ns] \$6,800 model: (1300nm) 4. **LaserDiode [0dBm, 0.60ns] \$2,495 model: LDDL-2100 (1300nm) 5. Tektronics [11.7dBm, 0.30ns] \$10,500 model: OIG502 (1300nm) 6. Tektronics [14.7dBm, 0.30ns] \$10,300 model: OIG501 (1300nm) 7. IPITEK [10dBm, 0.40ns] \$2,700 model: TX-500 (1300nm) 8. **SONY [6.99 dBm, 0.50ns] *** model: SLD-103U \$90 per 9. SONY [13 dBm, 0.50ns] model: SLD 201U/V \$90 per 10. SONY [14 dBm, 0.50ns] model: SLD 202U/V \$190 per 11. SONY [15 dBm, 0.50ns] *** model: SLD 203V \$180 for 3 12. SONY [16 dBm, 0.50ns] *** model: SLD 201U/V-3 13. SONY [20 dBm, 0.50ns] *** model: SLD 301V 14. SONY [23 dBm, 0.50ns] *** model: SLD 302V 15. SONY [26 dBm, 0.50ns] *** model: SLD 303V 16. SONY [30 dBm, 0.50ns] *** model: SLD 304V		

** Model not able to meet power requirements

*** Not available through distribution

**** Model not able to meet sensitivity requirements

***** Model not able to meet bandwidth requirements

Table 4-1c. Transceiver Candidates for M(16,4,7).

TRANSMITTER REQTS		RECEIVER REQTS		TRANSMITTER CANDIDATES/COST		RECEIVER CANDIDATES/COST	
P(dBm)	Tc	P(dBm)	Tc	S(dBm)	1/τc Bw	S(dBm)	1/τc Bw
13.4-18.4	1.85ns	13.4-18.4	1.85ns	11.7dBm, 0.30ns	\$10,300	14.7dBm, 0.30ns	\$10,300
3. SPR(16,4,7)				model: 0IG501 (1300nm)		model: MARX-DP	\$4,500
				2. Tektronix [11.7dBm, 0.30ns]	\$10,500	**** Opio Electronics [-23 dBm]	\$2,600
				model: 0IG502 (1300nm)		model: PAD-110	
				3. **IPITEK [10dBm, 0.40ns]	\$2,700	3. PCO [-29dBm]	\$4,200
				model: TX-500 (1300nm)		model: DRX-878	
				4. **SONY [6.99 dBm, 0.50ns]	***	4. LaserDiode [-27dBm]	\$1,000 per
				model: SLD-103U		model: LDPM-1000 (at 10 ⁻⁹ BER)	\$1,600 per
				5. SONY [13 dBm, 0.50ns]	\$90 per	5. BT & D [-30 dBm]	\$1,600 per
				model: SLD 201U/V		model: RCY 1201-1.2	
				6. SONY [14 dBm, 0.50ns]	\$90 per	6. Tektronix [will see 30ps]	\$45,525
				model: SLD 202U/V		model: SD46, SD30 & CSA803 Mainframe	
				7. SONY [15 dBm, 0.50ns]	\$190 per		
				model: SLD 203V			
				8. SONY [16 dBm, 0.50ns]	***		
				model: SLD 204V			
				9. SONY [20 dBm, 0.50ns]	***		
				model: SLD 301V			
				10. SONY [17 dBm, 0.50ns]	\$180 for 3		
				model: SLD 201U/V-3			
				11. SONY [20 dBm, 0.50ns]	***		
				model: SLD 301V			
				12. SONY [21 dBm, 0.50ns]	***		
				model: SLD 302V			
				13. SONY [26 dBm, 0.50ns]	***		
				model: SLD 303V			
				14. SONY [30 dBm, 0.50ns]	***		
				model: SLD 304V			

** Model not able to meet power requirements

*** Not available through distribution

**** Model not able to meet sensitivity requirements

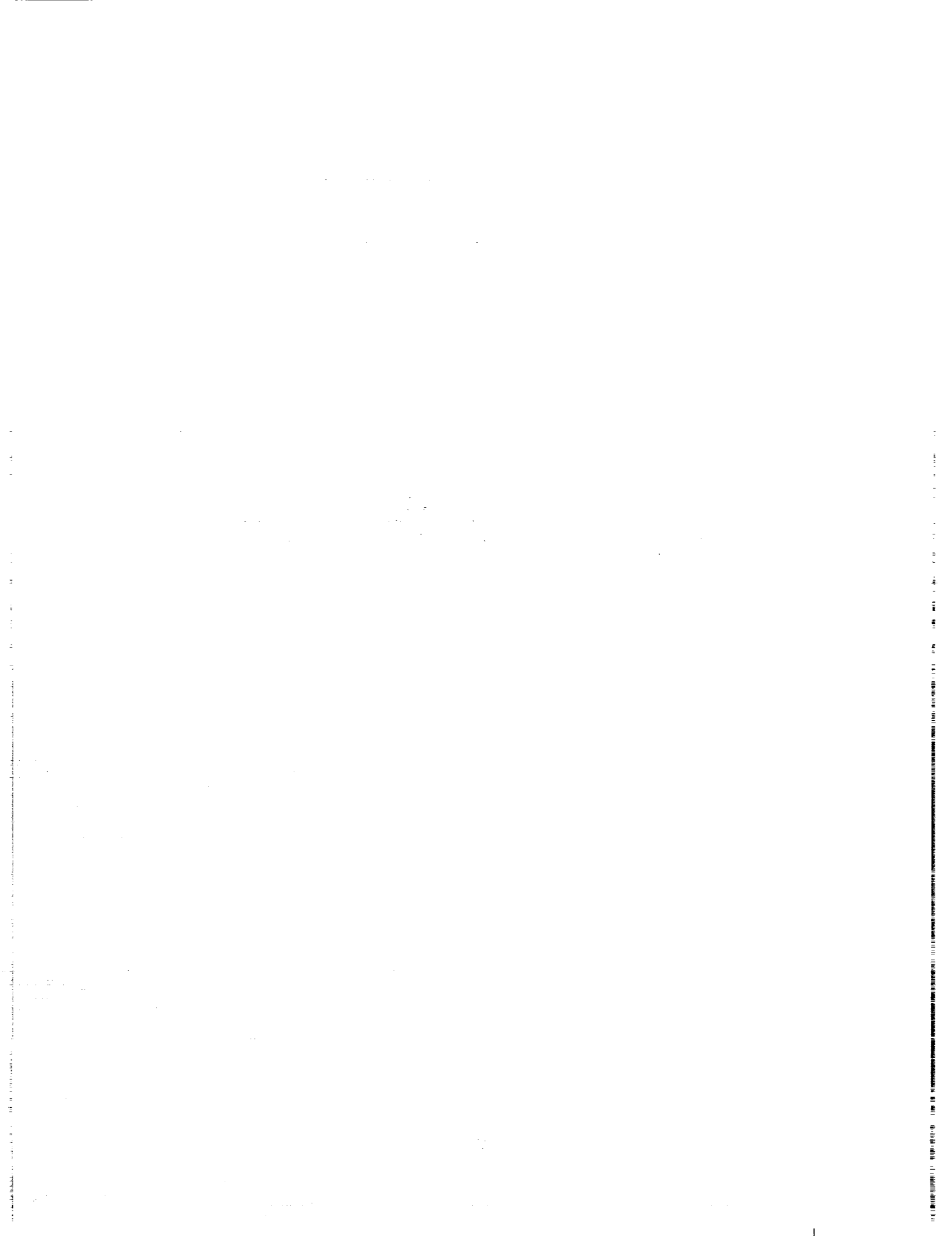
Trade Offs

The discussion given above can be used to structure a trade off matrix, as shown in Table 4-1.

Table 4-1. Photonic Networks Trade Off Matrix

Candidate	Data Rate	Affordable Components	Compatibility With ECC	Cost	Complexity	Growth Potential
(8,4,4)	1	1	1	1	1	1
(12,4,4)	1	2	1	2	2	1
(16,4,7)	1	3	1	3	3	3
Alternate (8,8,4)	1	2	Not Req'd	2	1	2

The ranking in the table is based on "1" being the best and "3" the worst. The criteria are based on the discussion in this chapter. We see from the table that, based on these quantitative and qualitative criteria, that the M(8,4,4) is the best candidate, followed by the alternate, M(8,8,4).



5.0 Selection of Preferred Candidate for Phase II and Refinement of Specifications

The previous chapters provide the background for selecting the preferred candidate for Phase II. This selection is the photonic network based on the $M(8,4,4)$ matrix codes.

System Description

The architecture of this photonic network is shown in Figure 5-1. The architecture includes 8 laser diode transmitters (T) which interface via a Circuit Interface Unit (CIU) with the satellite uplink. It also includes 8 $M(8,4,4)$ encoders, one for each transmitter. The eight encoders are based on two basic codes, the $M_1(8,4,4)$ and $M_2(8,4,4)$. All other codes are permutations of these two.

The encoder data is broadcast by means of 4 layered 8×8 stars. The layered stars interface with 8 decoders which are the inverses of the 8 encoders.

The output of the decoders (which consists of autocorrelation and superimposed cross correlation terms) is thresholded and detected by their respective receivers (R). The receivers interface with the satellite downlinks by means of the CIU.

On board routing or switching can be effected by reconfiguring the set of encoders on command of the Autonomous Network Controller. The mechanism for reconfiguring the encoders is further discussed in Chapter 9.0. All reconfigured encoders are M_1 , M_2 or a permutation of these two matrix codes.

The system operates at 180 Mb/s, point to point, with a BER of 10^{-3} uncorrected or 10^{-9} corrected (see Chapter 7.0).

Matrix Codes and Their Implementation

The selected 8 matrix codes are shown in Figure 5-2. M_1 (code #1) and M_2 (code #5) are both derived from folding a (0,1) pulse sequence pseudo orthogonal code, with the added constraint of a single pulse per row.

The columns of the matrices are unit delays (chip times). The rows are the space channels which are broadcast by the layered stars. The column position of the "1", or pulse, in the matrices indicates the time delay required in that row. Note that all matrices have at least one pulse in column one, which assists in timing and clock recovery. Note, also, that the maximum delay is 6 chip times, corresponding to 6 columns.

The photonic implementation of these matrix codes is shown at the top of Figure 5-2. A single pulse from T, having a pulsewidth T_c and corresponding to an electrical bit of bit time T_b , is split into four synchronous pulses of equal peak power by a 1×4 splitter.

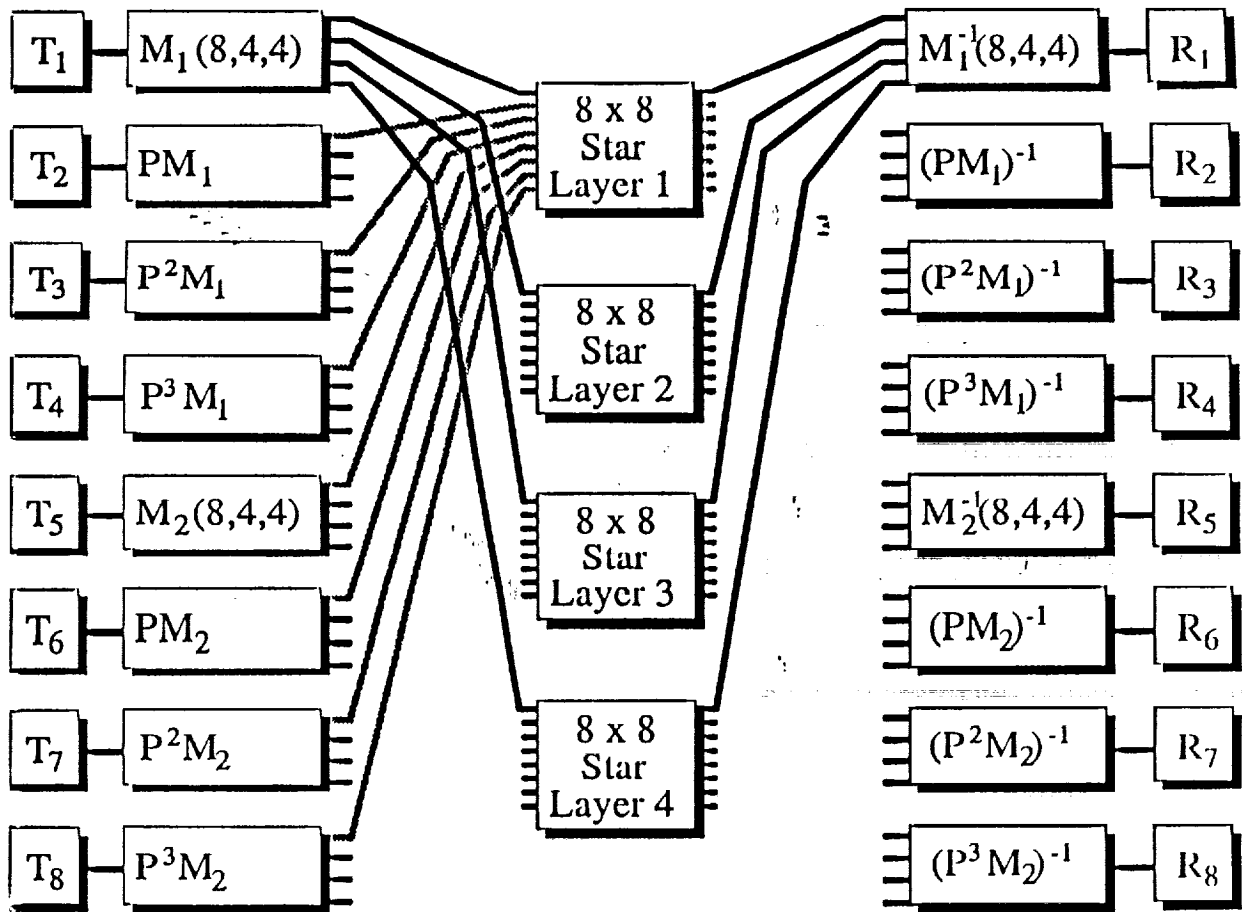


Figure 5-1.

Architecture of Preferred Candidate Photonic Network

$M_i(N, w, f)$	= matrix code i
$P^n M_i$	= n^{th} permutation of matrix M_i
M_i^{-1}	= inverse of matrix code i ("optical correlator")
$(P^n M_i)^{-1}$	= inverse of matrix code $P^n M_i$
T_j	= transmitter j
R_k	= receiver k

6/20/91

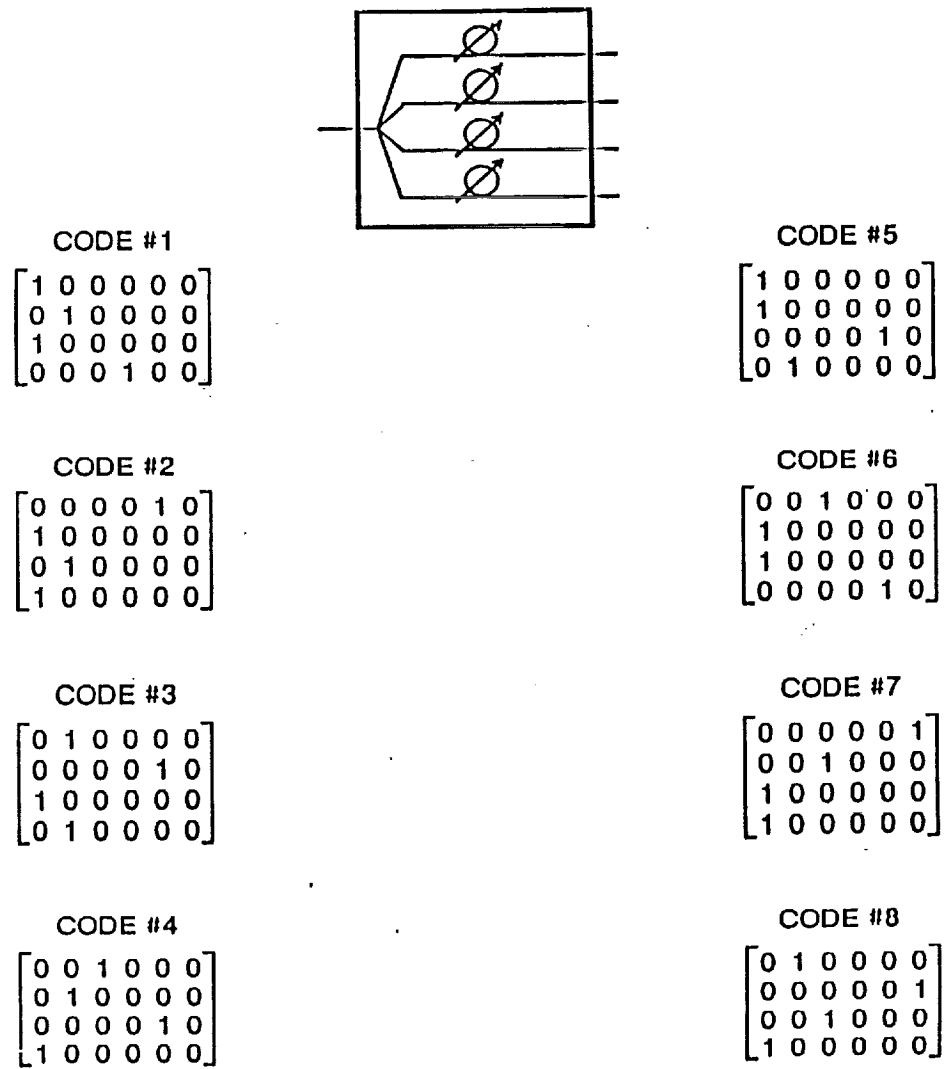


Figure 5-2. CDMA Matrix Codes and Their Fiber Optic Implementation.

The four arms of the splitter correspond to the four space channels. Each space channel is then delayed by means of a fiber optic delay line according to the code prescription. The four delayed pulses are then broadcast by the layered stars: layer 1 broadcasts row 1, layer 2 broadcasts row 2, etc.

On the receiver side, row 1 of each decoder is attached to layer 1, row 2 to layer 2, etc. The decoders add delays on a row by row basis according to their prescription. The output of these rows are optically summed by a 4x1 combiner. This optically summed output is converted to an electrical signal by means of a photodetector. The output of the photodetector is thresholded and detected. A threshold crossing reconstructs an electrical "1" of bit time T_b ; non crossing reconstructs a "0" bit of bit time T_b .

Refinement of Specifications

Based on the vendor survey, the laser peak power and receiver sensitivity requirements were modified as discussed in Chapter 4.0. If ECC is used, then the channel data rate and bit time (and chip time) need to be similarly modified, as discussed in Chapter 7.0. The refined specifications are shown in Table 5-1.

Chapter 6.0 gives the bill of materials which would be sufficient for integrating and assembling the preferred candidate.

Table 5-1. Refined Specifications for Preferred Candidate

Matrix	Laser Pulsewidth (T_c) and Data Rate	Transmitter Peak Power	Receiver Sensitivity
M(8,4,4)	0.93 ns @ 180 Mb/s without ECC	8-13 dBm	-27 dBm (PIN) @ $1/T_c$ Bandwidth
	0.65 ns @ 256 Mb/s with ECC		

Alternate Design

The alternate design, selected because it minimizes the dependence on ECC, is shown in Figure 5-3. Note that the photonic network fabric is identical to the preferred selection. The only difference is in the weight of the codes (8 instead of 4) which shows up as two pulses per row rather than a single pulse per row. The weight eight matrices have more columns, so the chip time is consequently shorter. The laser transmitter T, then, has shorter pulses and higher peak power. The laser receiver must detect these shorter pulses. Thus, the alternate design obviates the requirements for ECC while requiring more complex and/or expensive transceivers.

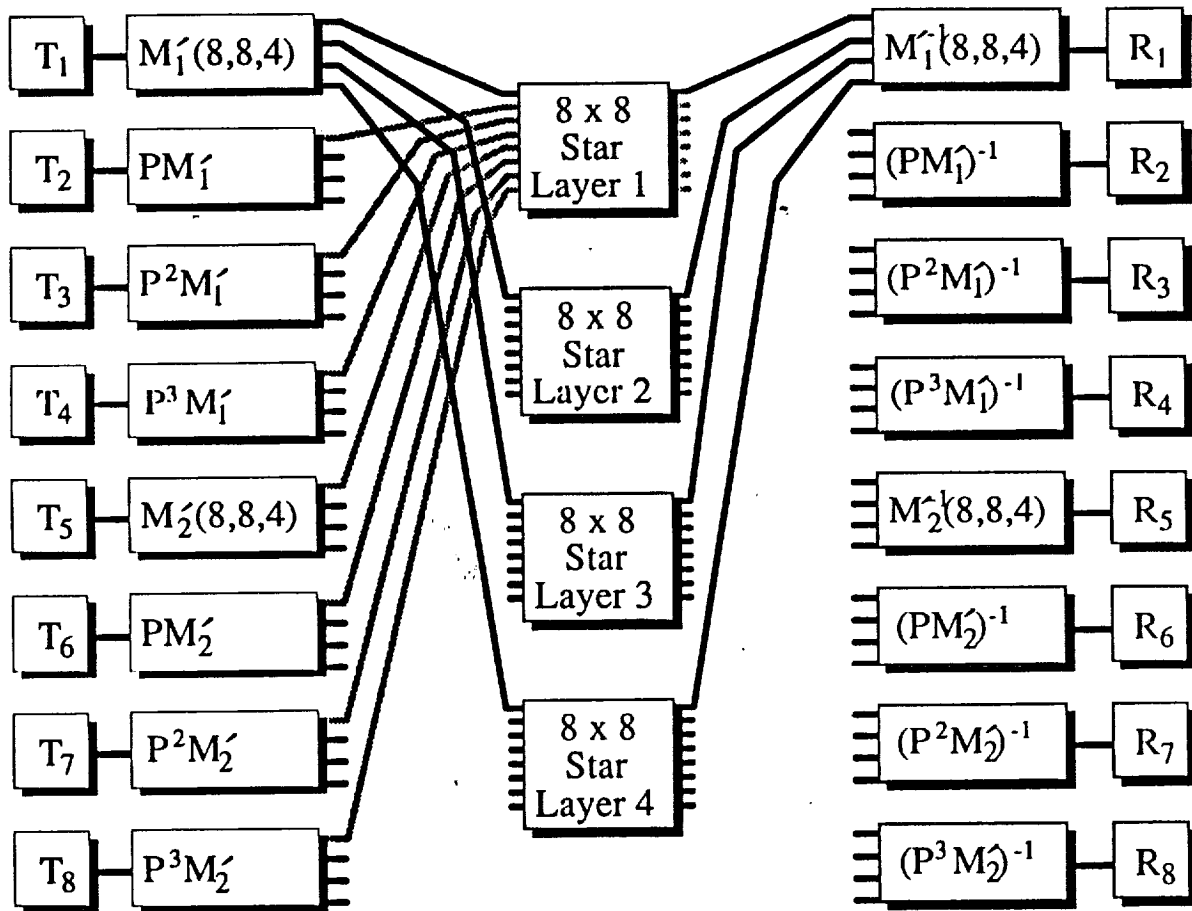


Figure 5-3.

Architecture of Alternative Candidate Photonic Network

$M_i'(N,w,f)$	= alternative matrix code i
$P^n M_i'$	= n^{th} permutation of matrix M_i'
$M_i'^{-1}$	= inverse of matrix code i ("optical correlator")
$(P^n M_i')^{-1}$	= inverse of matrix code $P^n M_i'$
T_j	= transmitter j
R_k	= receiver k

7/03/91

6.0 Bill of Materials of Preferred Candidate

The following is a list of items required to construct the fabric for an eight user, weight four, with four space channels (M(8,4,4)) temporal/spatial CDMA network.

- (1) 8 Encoders: 8 - 1x4 bidirectional couplers
- (2) 8 Decoders: 8 - 1x4 bidirectional couplers
- (3) Broadcasting: 4 - 8x8 star couplers
- (4) Miscellaneous fibers and connectors

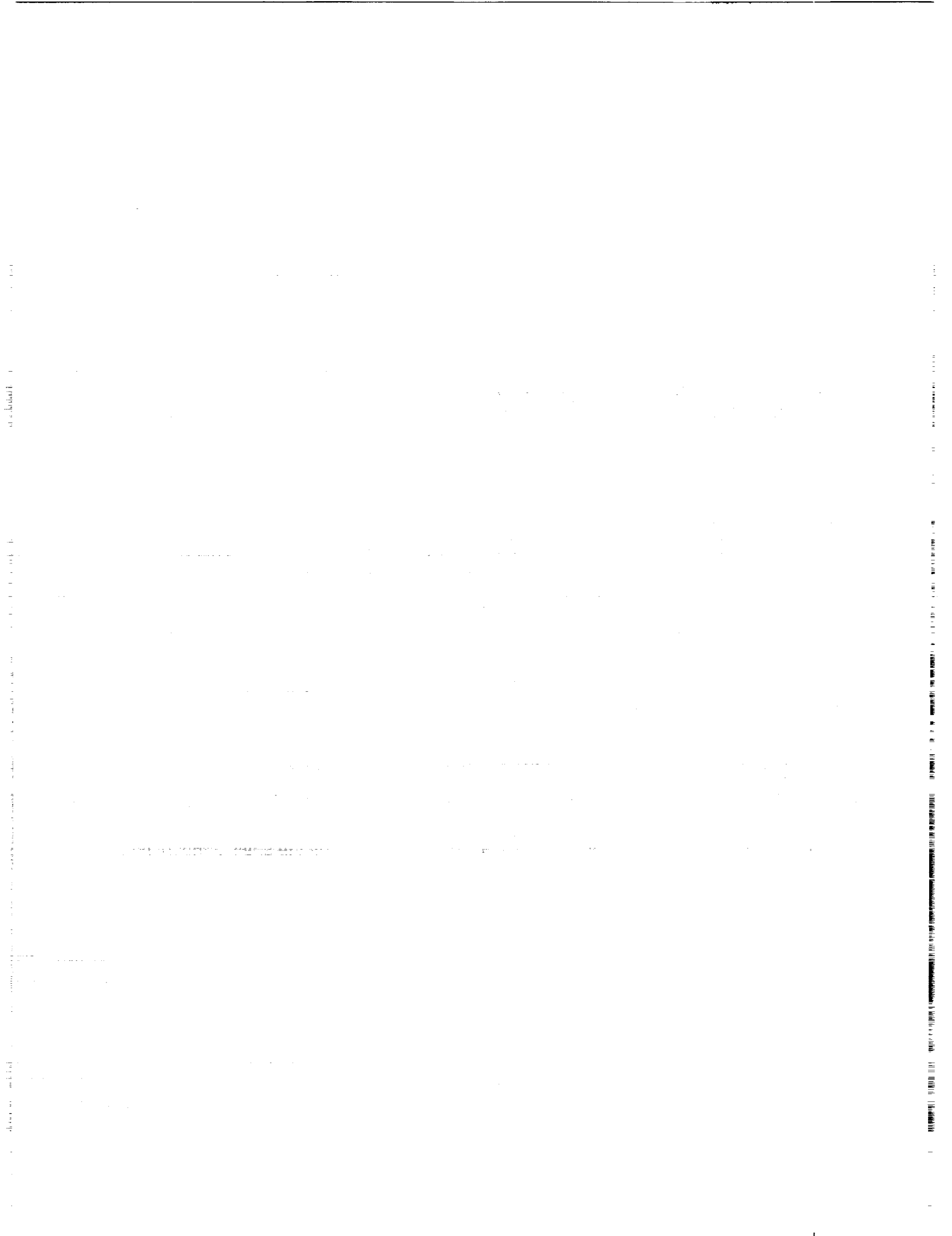
The active components required are

- (5) 8 laser drivers capable of driving a laser diode at 180 Mb/s (without Error Correction Codes, ECC) or 256 Mb/s (with ECC). (See next chapter.)
- (6) 8 laser diodes capable of 0.93 ns @ 180 Mb/s (without ECC) or 0.65 ns @ 256 Mb/s (with ECC), 8-13 dBm
- (7) 8 receivers with -27 dBm sensitivity for 0.93 ns (without ECC) or 0.65 ns (with ECC).

All of these passive and active components are off the shelf. The ECC chip (RS(54,38,8,)), if required, also is off the shelf.

The bill of materials does not make provisions for reconfigurable encoders/decoders, nor does it include peripheral equipment and special test equipment.

The alternate solution, M(8,8,4), also can be constructed with off the shelf components.



7.0 Bit Error Rate Analysis of Preferred Candidate and Applicable Error Correction Codes and Alternatives

The build-up of crosstalk interference (which we shall call clutter) in any one CDMA channel due to multiple concurrent communications may produce decoding errors that may not be tolerable, depending on system requirements. We have made some analytical estimates and carried out computer modeling to quantify the effects of clutter. Several preliminary concepts were investigated to determine if they could reduce the effects of the clutter, should this be required. The preliminary concepts considered were:

- error correction coding
- block waveform encoding (PPM)
- adaptive thresholding

Each of these approaches indeed improves the operating bit error probability (P_b) of the overall links, as shown below.

Error Correction Coding

With error correction encoding, a level of electronic processing is inserted before and after the optical interconnect, as shown in Figure 7-1. The electronic processing corresponds to converting the input electronic data bits to binary code symbols (called channel encoding), which are then transmitted as optical bits. After decoding the recovered channel symbols (with error caused by clutter) these are then converted back to the data bits via the electronic channel decoding. With properly selected channel coding, the reconstructed output bits will have fewer errors (the coding has corrected some of the symbol transmission errors), thereby improving the overall bit error rate (BER).

Error correction is accomplished within the coding by the insertion of redundant symbols that aid in identifying the symbol errors after transmission. However, this means the optical symbol rate must be faster than the input bit rate. This in turn means either the bit rate must be reduced if the optical channel can only handle a specific symbol rate, or the optical rate (as determined by the sequence sets and pulse chip

time) must be increased above the bit rate. The ratio of available optical symbol rate to the desired input bit rate is called the coding margin. With a required input bit rate of 180 Mb/s, analytical results to date show that a coding margin of about 2 reduces the raw BER by many orders of magnitude. We also find that the electronic technology exists which lets this coding margin be feasible for our application. Many types of well-established coding techniques (e.g., Reed-Solomon (RS) block codes, rate 1/2 convolutional codes) operate quite well at this margin.

A study was carried out to examine the potential improvement in bit error probability P_b by inserting this channel coding into each CDMA link. This was determined by first computing the uncoded bit error probability using estimated values of the link parameters. The procedure was to determine the post detection SNR after CDMA decoding, taking into account the effects of CDMA losses, shot noise, detector noise, thermal noise, and clutter. Assuming Gaussian noise statistics and using a threshold adjusted so that the bit error probability when sending ones and zeros was balanced, the resulting uncoded bit error probability of a single CDMA channel can be written as

$$P(E) = Q \left(\frac{\frac{K_s}{Nw^3}}{\sqrt{\left(\frac{K_s}{Nw^3} + \frac{K_s}{2Nw^4} \left(\frac{N-1}{N}\right)\right)F + \frac{K_s^2}{2N^2w^8} \left(\frac{N-1}{N}\right) + \frac{K_n}{(G)^2}} + \sqrt{\frac{K_s^2}{2N^2w^8} \left(\frac{N-1}{N}\right) + \frac{K_n}{(G)^2}} \right)} \right) \quad (7-1)$$

where K_s and K_n are the signal and noise electron counts, N the size of the network (number of users), w the weight of the code, G the detector (PIN or APD) gain, F the excess noise factor and Q the Q function. This expression holds for PIN and APD receivers. Implicit in K_s and K_n are the detector quantum efficiency, the wavelength, and the chip time T_c .

For simplicity, Gaussian statistics have been assumed in order to generate some preliminary estimates. (The computer simulations discussed in Chapter 4 indicated that the statistics are not Gaussian, but skewed. Further improvements in the theory should take this into account.) With this raw P_b determined, the resulting coded bit error probability can be estimated by converting the link optical symbol error

probability to the data bit error probability after channel decoding. Figures 7-2 to 7-5 show the resulting P_b for an uncoded and an RS code link versus required laser power; $N = 8$ in all cases. Figure 7-2 is for a linear CDMA sequence set with a weight = 4, while Figure 7-3 is for a matrix CDMA set with weight 4, $f = 4$ (i.e., the selected design). Figures 7-4 and 7-5 show the same analyses for weight = 8 codes; Figure 7-4 is for the linear CDMA case and Figure 7-5 for the alternative matrix CDMA design. In each case the potential improvement effected by the coding is remarkable and apparent.

The Reed Solomon code RS(54, 38, 8), which is commercially available, was used in the computations. Therefore, the curves labeled "RS" have assumed a channel bit rate of $(54/38) \times 180$ Mb/s, or 256 Mb/s, and a channel chip time of $(38/54) \times T_c$.

Figures 7-2 through 7-5 assume that the optimal threshold is used (see Adaptive Threshold discussion, below).

PPM Signaling

An alternative to binary channel coding is the use of pulse position modulation (PPM) to improve performance. In this case electronics is inserted that partitions the input bits into k bit blocks that are then transmitted as an optical PPM waveform (single laser pulse in one of the $M=2^k$ possible positions, as in Figure 7-6). If all CDMA channels use this same format, the PPM block encoding has the effect of reducing the inter-channel crosstalk by spreading it over the total M -position frame, thereby reducing the chances of clutter build up. The overall result is to improve the link bit error probability.

Figure 7-7 shows the expected improvement in P_b as PPM of various levels is inserted. The system has the advantage that the optical pulse rate is reduced from the input bit rate. Hence PPM is advantageous whenever the optical link cannot handle the symbol rate required by an error correction coded system, or if the electronic channel coder cannot operate at the input bit rate. The effective chip time which the system must handle is $(1/\log_2 M) \times T_c$.

Adaptive Threshold

The previous analyses were based on the assumption of Gaussian interference. Situations exist, however, where the crosstalk will have a repetitive nature to it, producing interference levels that may repeat during data transmission. This suggests some level of improvement in P_b may be possible simply by properly setting the decoding threshold above the clutter floor. By observing a particular CDMA channel during a time period when a controlled data sequence is sent, crosstalk levels may be estimated and used to model the subsequent interference level for the remaining transmission period. This would permit optimal adjustment of the optical decoding threshold (Figure 7-8) to produce the minimal P_b (see Figure 7-8 corresponding to $L(8, 4)$ and Figure 7-10 corresponding to $L(8, 8)$). Note that the minimum is relatively deep and relatively narrow, so that it is important to operate close to this threshold setting. The adaptive threshold technique would locate and lock to this setting. This alternative merits further investigation and research, especially in conjunction with either ECC or PPM methods.

Figures 7-9 and 7-10 are plotted vs. the normalized threshold nTh which is defined as

$$nTh = \begin{bmatrix} Th - I(0) \\ I(w) - I(0) \end{bmatrix} \quad (7-2)$$

where

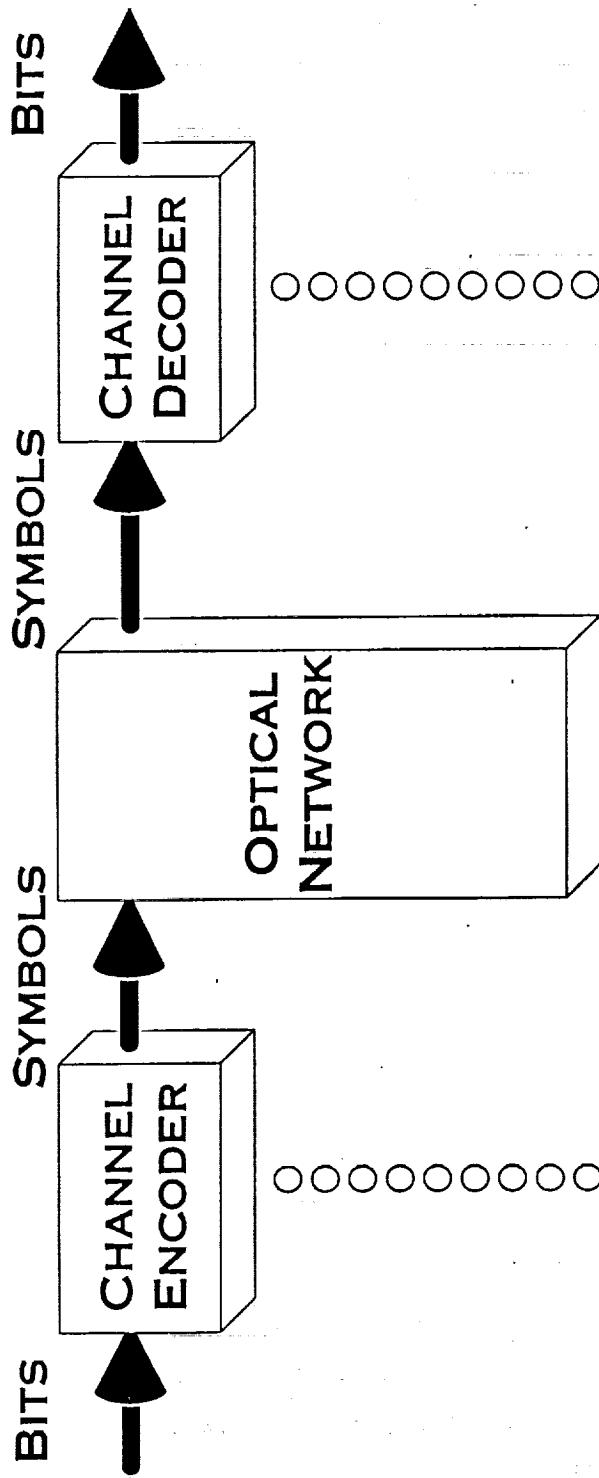
$I(0)$ = mean current ("0" pulses received, no interference from other users)

$I(w)$ = mean current when "1" pulse of weight w is received with no interference from other users

The curves in Figure 7-9 and 7-10 show the variation of P_b with normalized threshold for the particular sets of CDMA system parameters corresponding to $L(8, 4)$ and $L(8, 8)$, respectively. The curves show that a threshold setting which is too low will increase the zero ("0") bit errors, while too high a threshold increases the one ("1") bit errors. An optimal threshold, balancing these bit errors, produces the minimal P_b . Note from the figures that the optimal threshold depends on the CDMA system parameters, as well as the number of concurrent users. Since the threshold setting is related to the clutter and noise, an updated measurement of the channel interference level can be used to continuously drive the system to operate at the minimal P_b . Further study is needed to determine the accuracy to which the clutter can be estimated in a fixed time interval.

BIT ERROR CORRECTION

Figure 7-1.



$$\text{CODE FACTOR} = \frac{\text{SYMBOL RATE}}{\text{BIT RATE}}$$

Figure 7-2.
 Pb vs laser power: single fiber OOK
 $w=4, N=8, T_c=110$ ps
 $G=20, F=8$

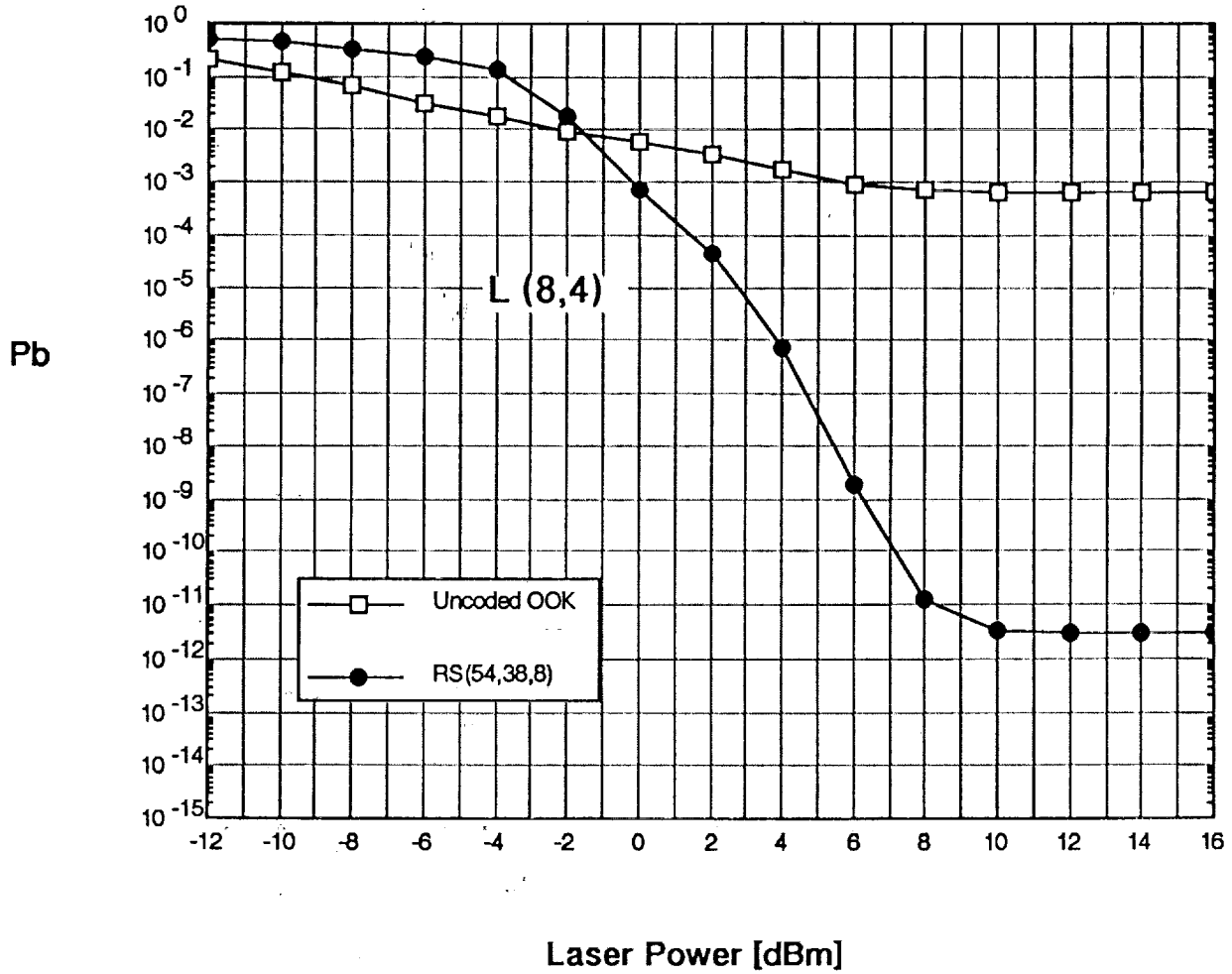


Figure 7-3.

Pb vs laser power: OOK, 4 - fibers

w=4 (assumed 1 pulse per fiber), N=8

Tc=900, G=1, F=1

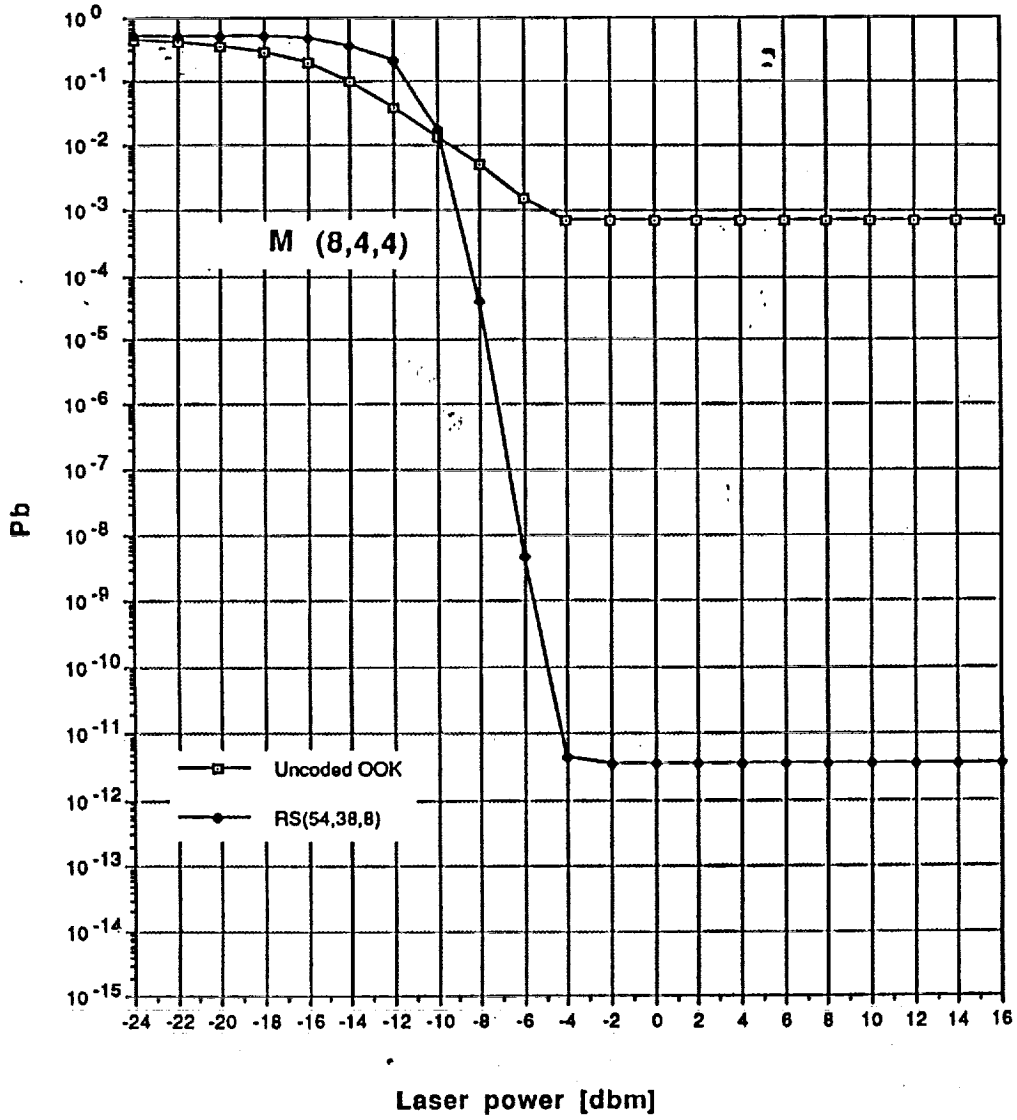


Figure 7-4.
 Pb vs laser power: single fiber OOK
 $w=8, N=8, T_c=25$ ps
 $G=20, F=8$

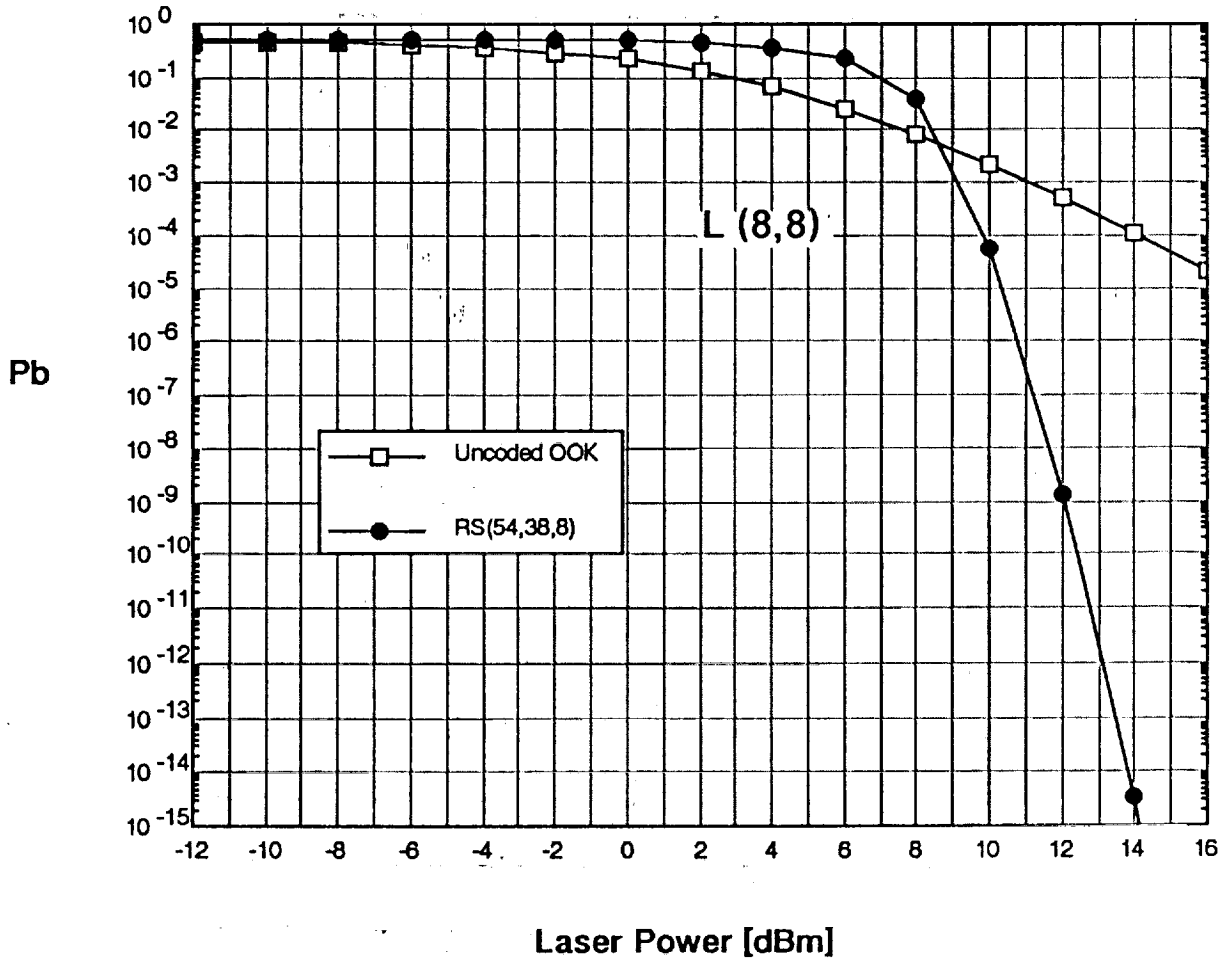


Figure 7-5.
 Pb vs laser power: OOK, 4 fibers
 $w=8$ (assumed 2 pulses per fiber), $N=8$
 $T_c=300$, $G=1$, $F=1$

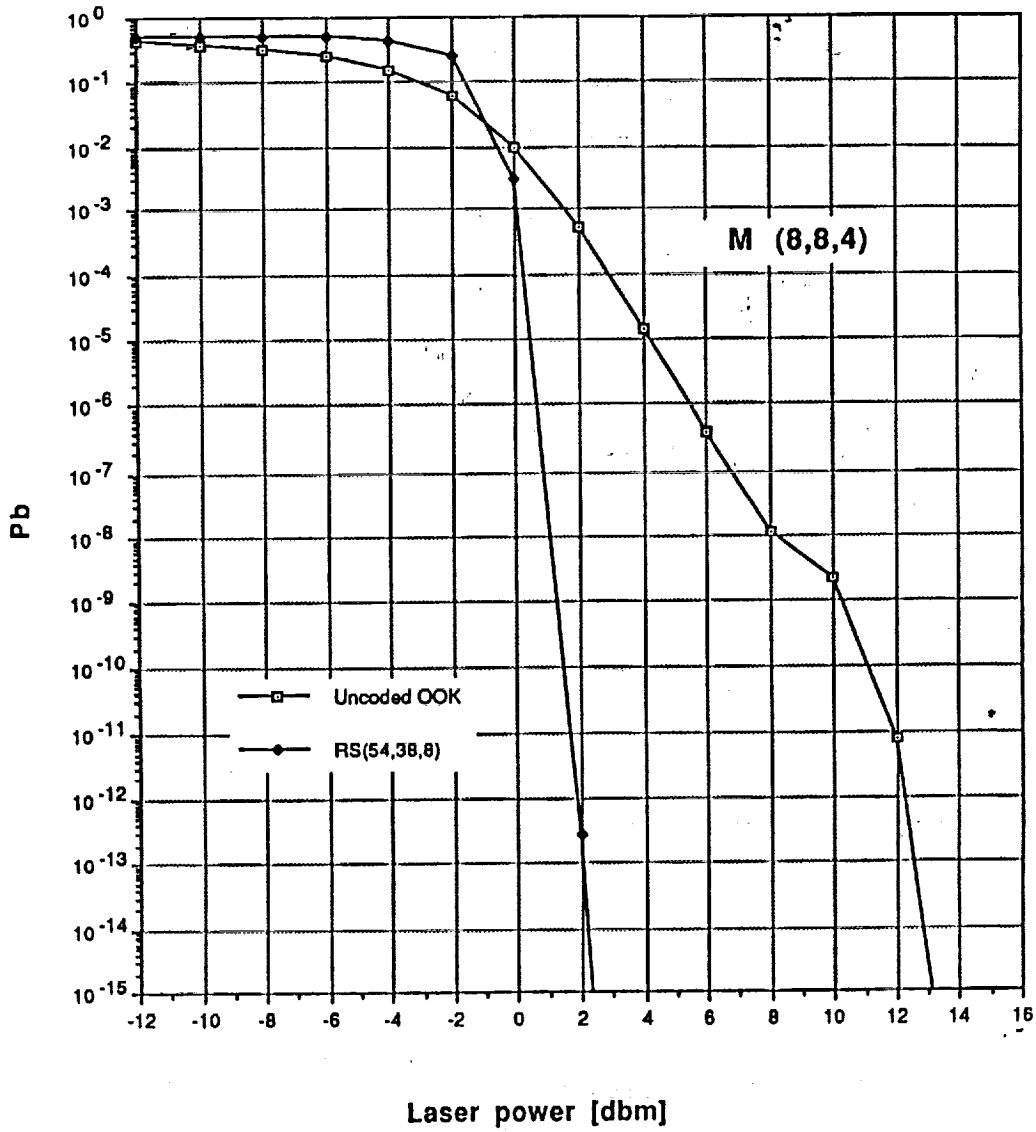
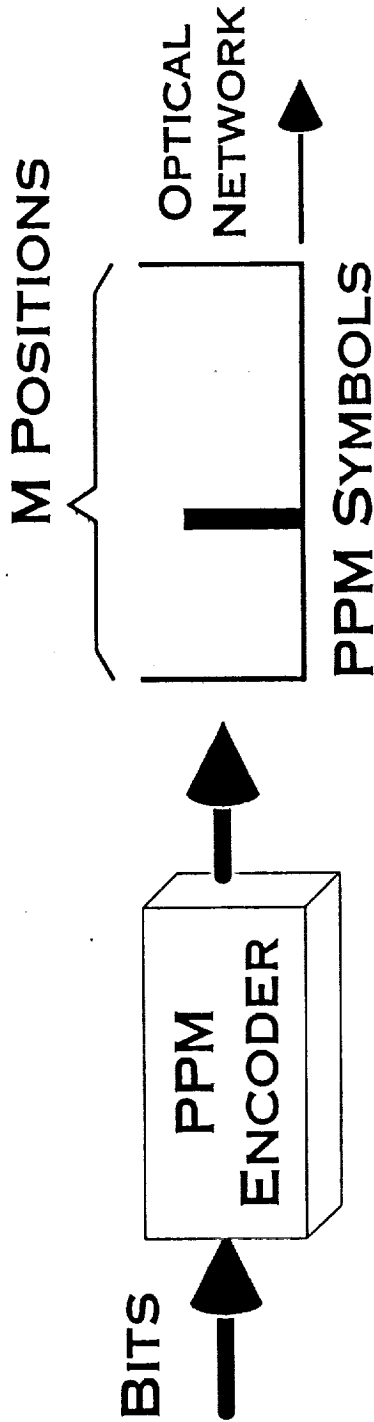


Figure 7-6.

CODED WORDS (PPM)



$$\text{CODE FACTOR} = \frac{1}{\text{LOG}_2 M}$$

Figure 7-7.

Avg Pb vs laser power: PPM single fiber (upper bound)

$w=4, N=8, G=20, F=8$

T_c : (OOK=110, 4-PPM=55, 8-PPM=37, 16-PPM=25) ps

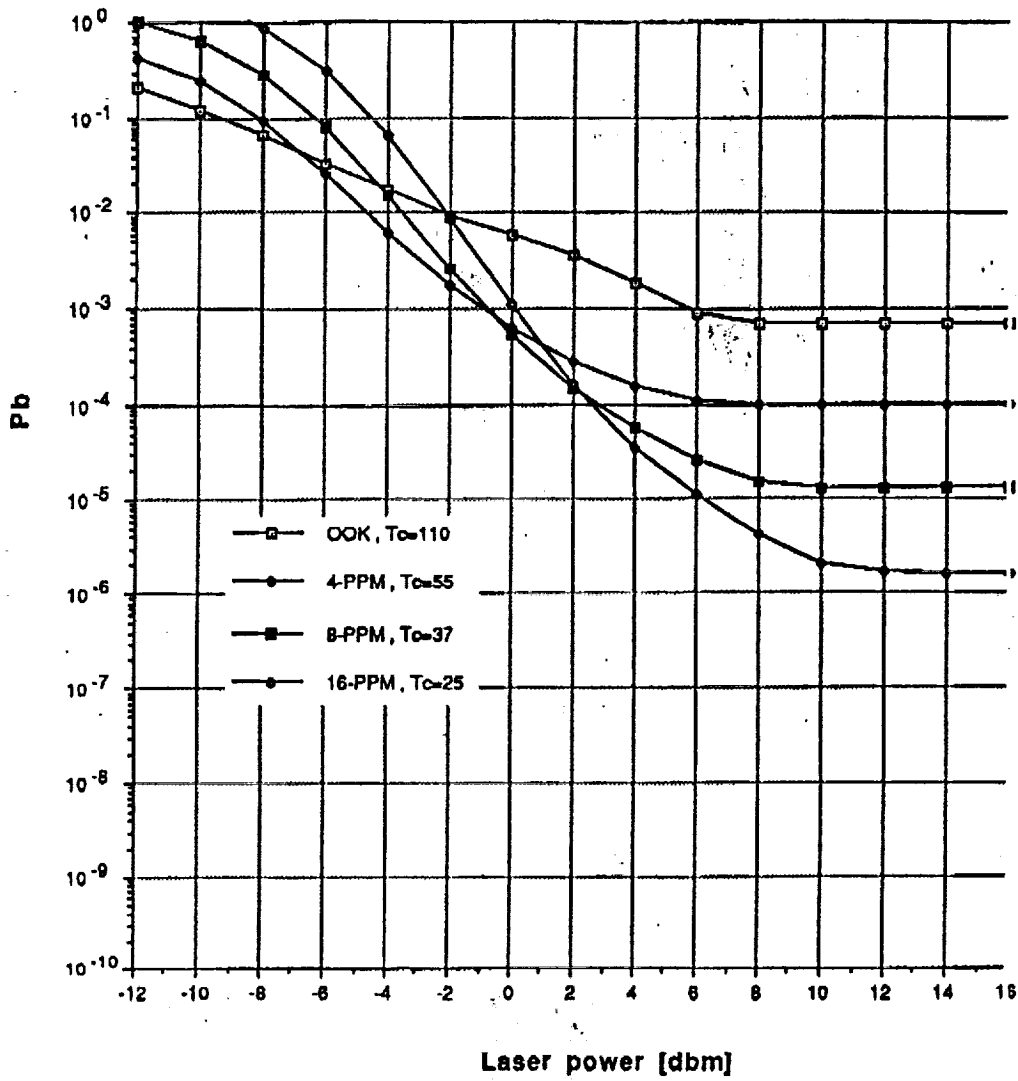


Figure 7-8.

THRESHOLD ADJUSTMENT

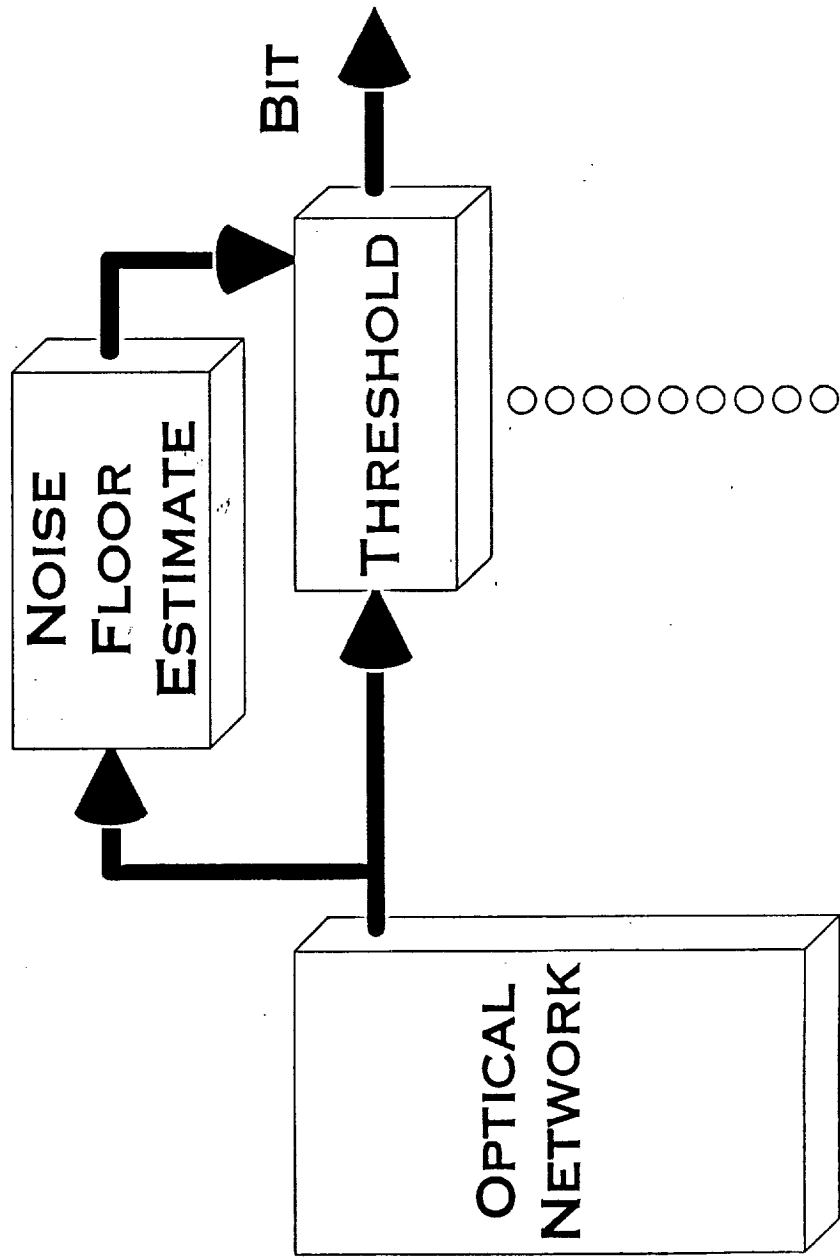


Figure 7-9.
Average Pb vs normalized threshold:
 $w=4$, $N=8$, $T_c=110$ ps, $G=20$, $F=8$
 $P_t = 8$ dbm, single fiber

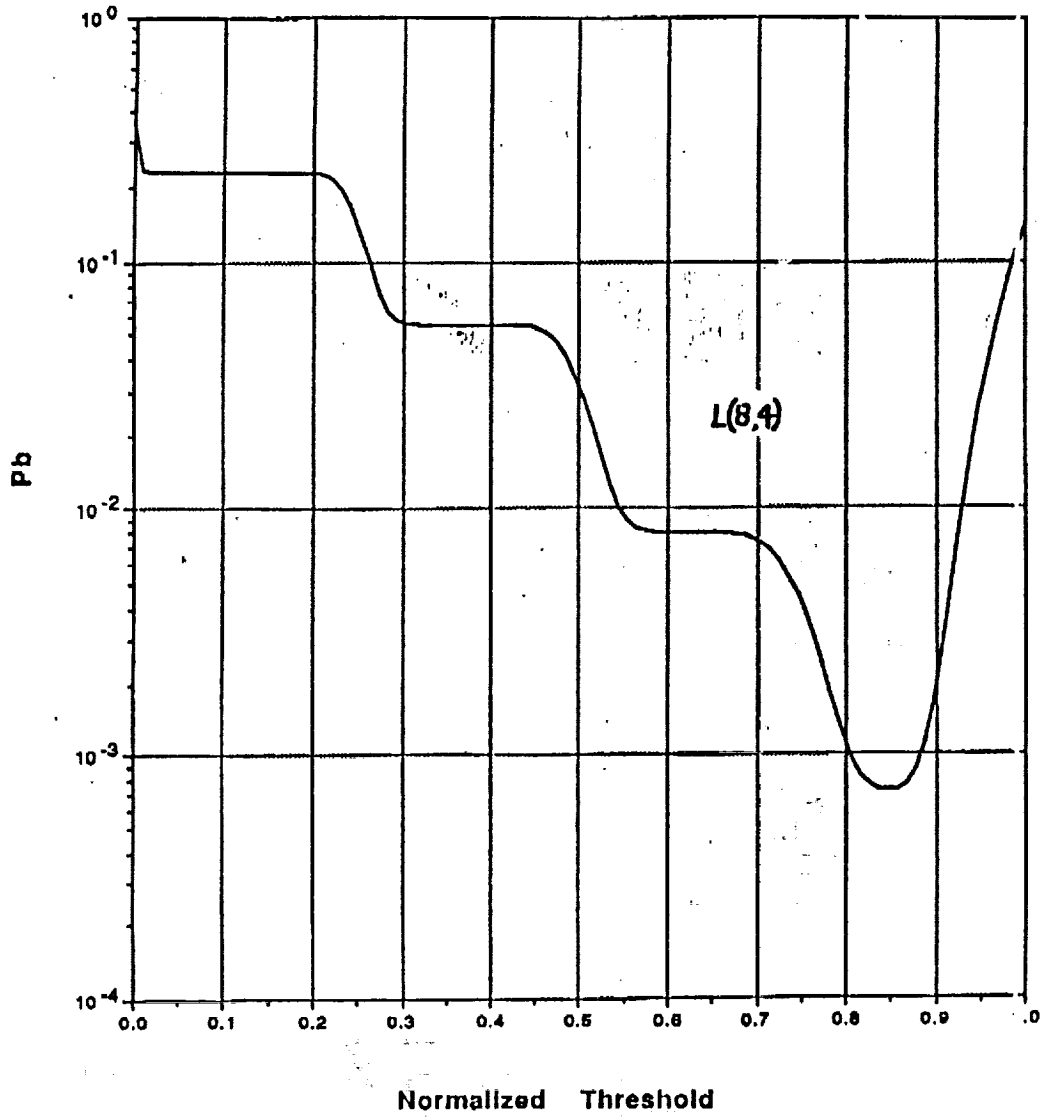
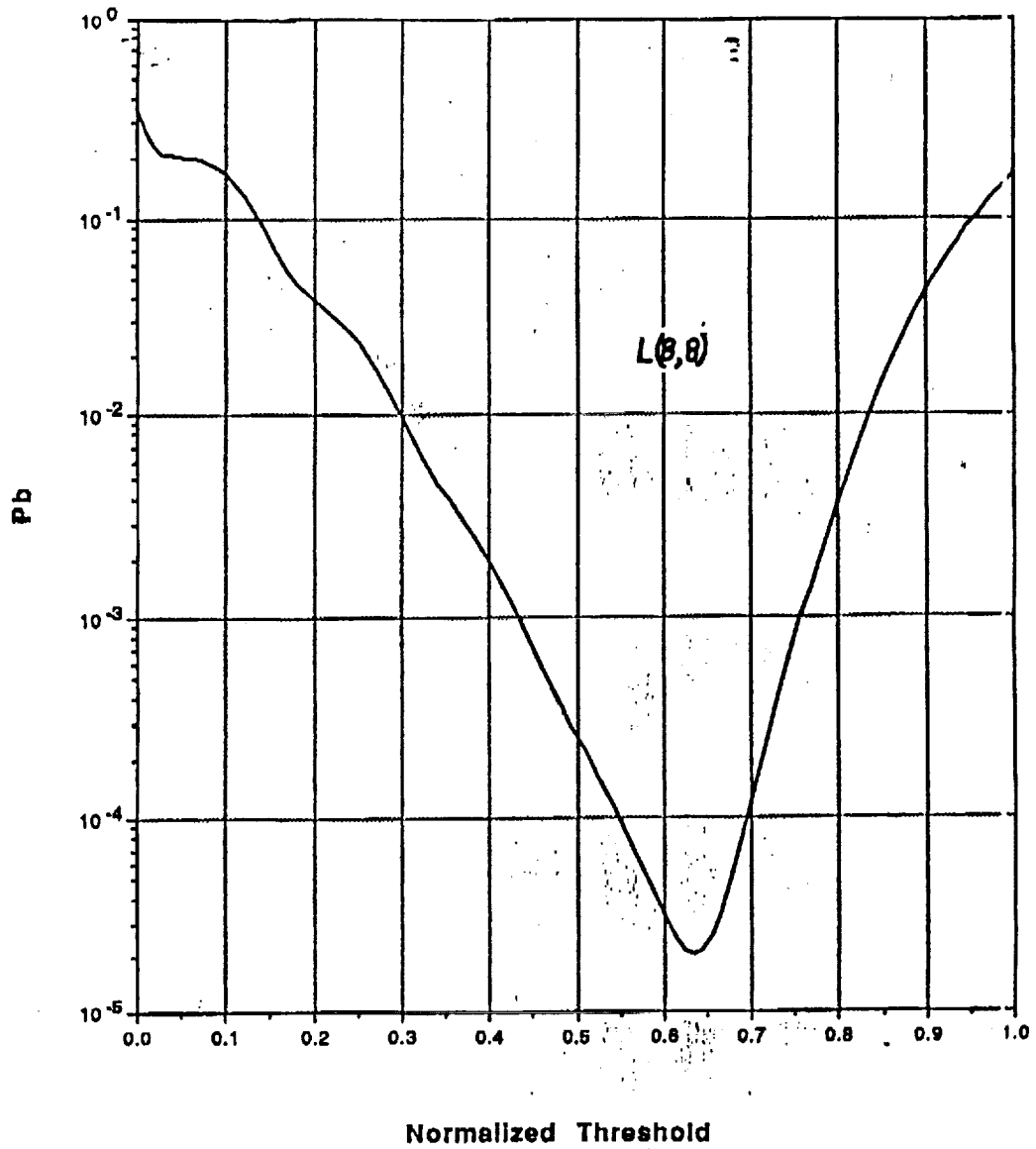
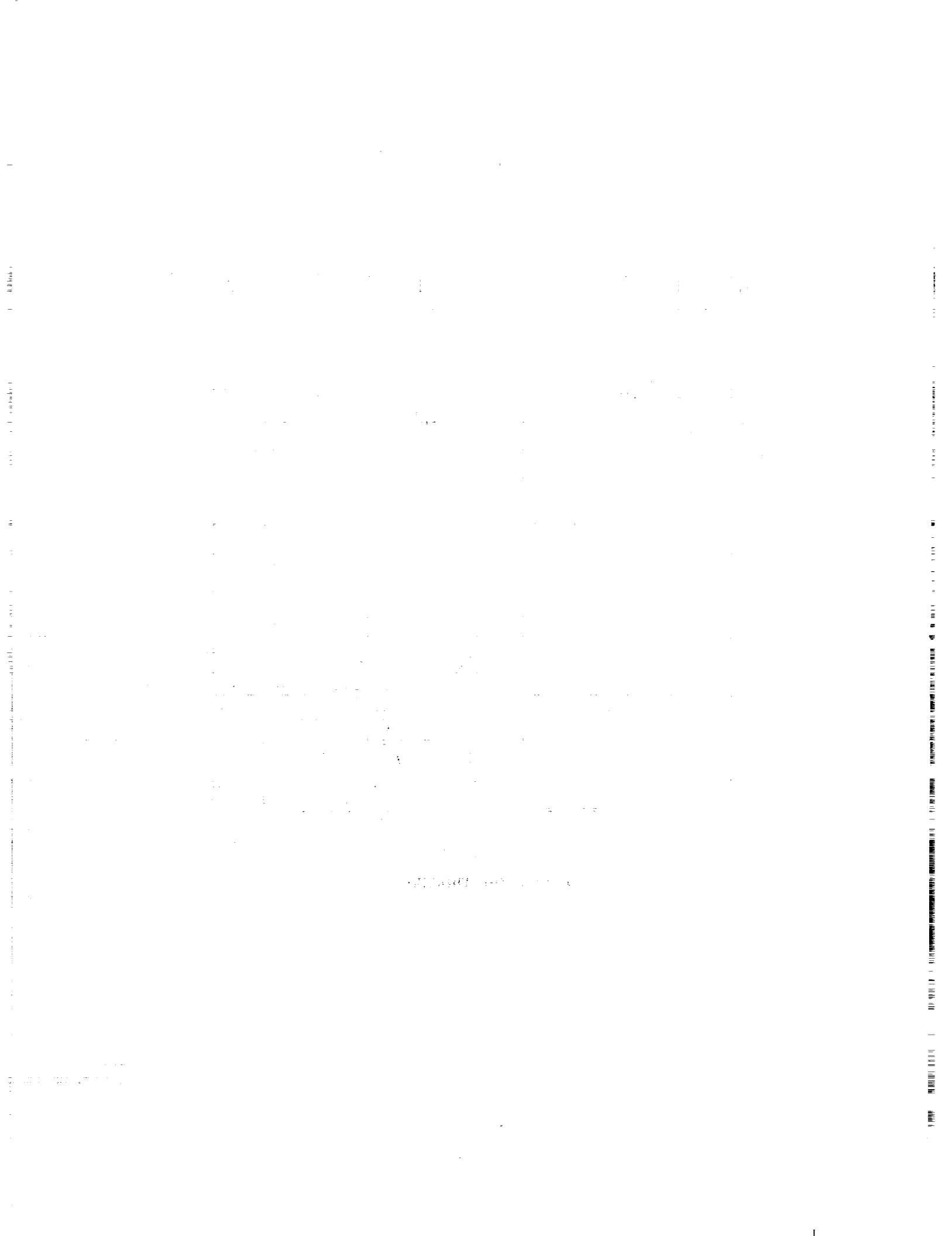


Figure 7-10.
Average Pb vs normalized threshold:
 $w=8, N=8, T_c=25 \text{ ps}, G=20, F=8$
 $P_t = 16 \text{ dbm}$, single fiber





8.0 Demonstration and Evaluation of Subscale Temporal and Temporal/Spatial CDMA Networks

A subscale breadboard was designed and built to demonstrate and evaluate a four-user, weight four optical CDMA network. This breadboard is capable of implementing either temporal CDMA or temporal/spatial CDMA. The following describes the experimental set-up and results.

The breadboard consisted of 10 1x4 fiber couplers and 4 4x4 fiber star couplers. All fibers including the delay lines were 62.5/125 multimode graded-index fibers with effective refractive index of 1.5. An optical time domain reflectometer (OTDR) in transmission mode was used to evaluate the breadboard (see Figure 8-1). The OTDR laser transmitter had a FWHM pulsewidth of approximately 100ps with 200mW peak pulse power, and the detector was an APD with sensitivity down to -27dBm. To increase the SNR of the detector, a processing unit associated with the OTDR was used to sample and average the detector output.

The chip time T_c was chosen to be 400ps, which corresponds to a fiber length of 8cm.

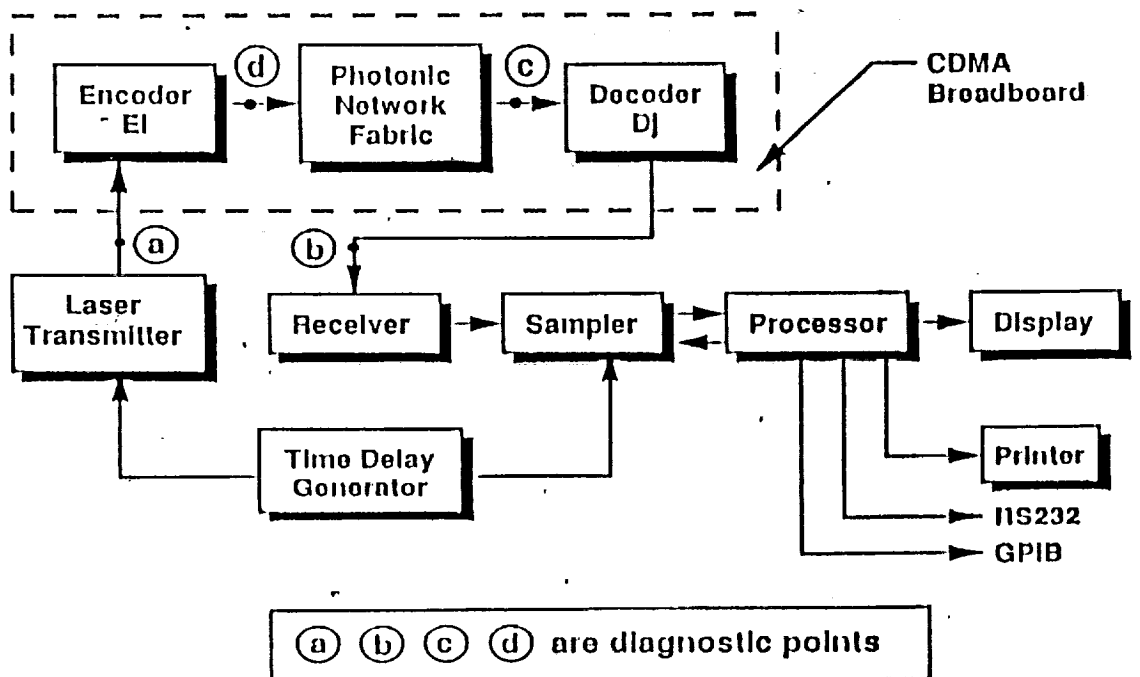


Figure 8-1. Diagram of Experimental Set-up.

Temporal CDMA

A code set for four users, weight four (L(4,4)) was implemented using fiber optic delay lines. Figure 8-2 shows the breadboard architecture and Figure 8-3 shows the code assigned to Encoder #1 (User #1) and pulse representation. The total length of the coupler pigtail and the delay line is indicated. The decoder was chosen to match Encoder #1.

Figure 8-4 shows the decoder output when only one user is transmitting at a time. Figures 8-5 and 8-6 show the decoder output when Encoder #1 and others are simultaneously transmitting (multi-user interference or MUI). The first case (Fig. 8-5) is the bit-synchronous MUI where all users are sending a "1" bit in synchronism. The second case (Fig. 8-6) is the "worst-case" MUI where Users #2-4 have their bits delayed in time with respect to User #1's bit resulting in the crosscorrelation terms lining up with the autocorrelation sidelobes so that the clutter has strong spikes which compete with the autocorrelation peak.

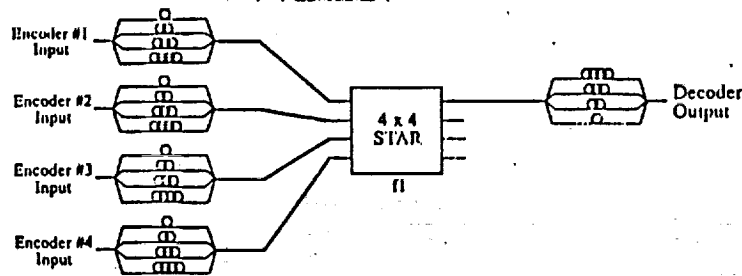


Fig. 8-2. Breadboard architecture for temporal CDMA.

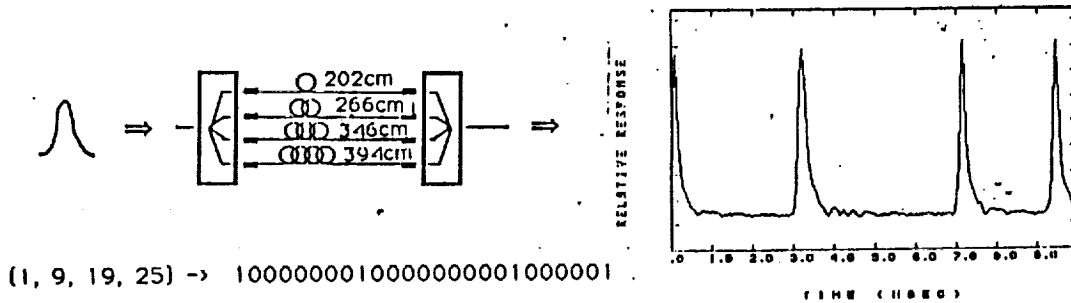


Figure 8-3. User #1's code, encoder, and pulse representation.

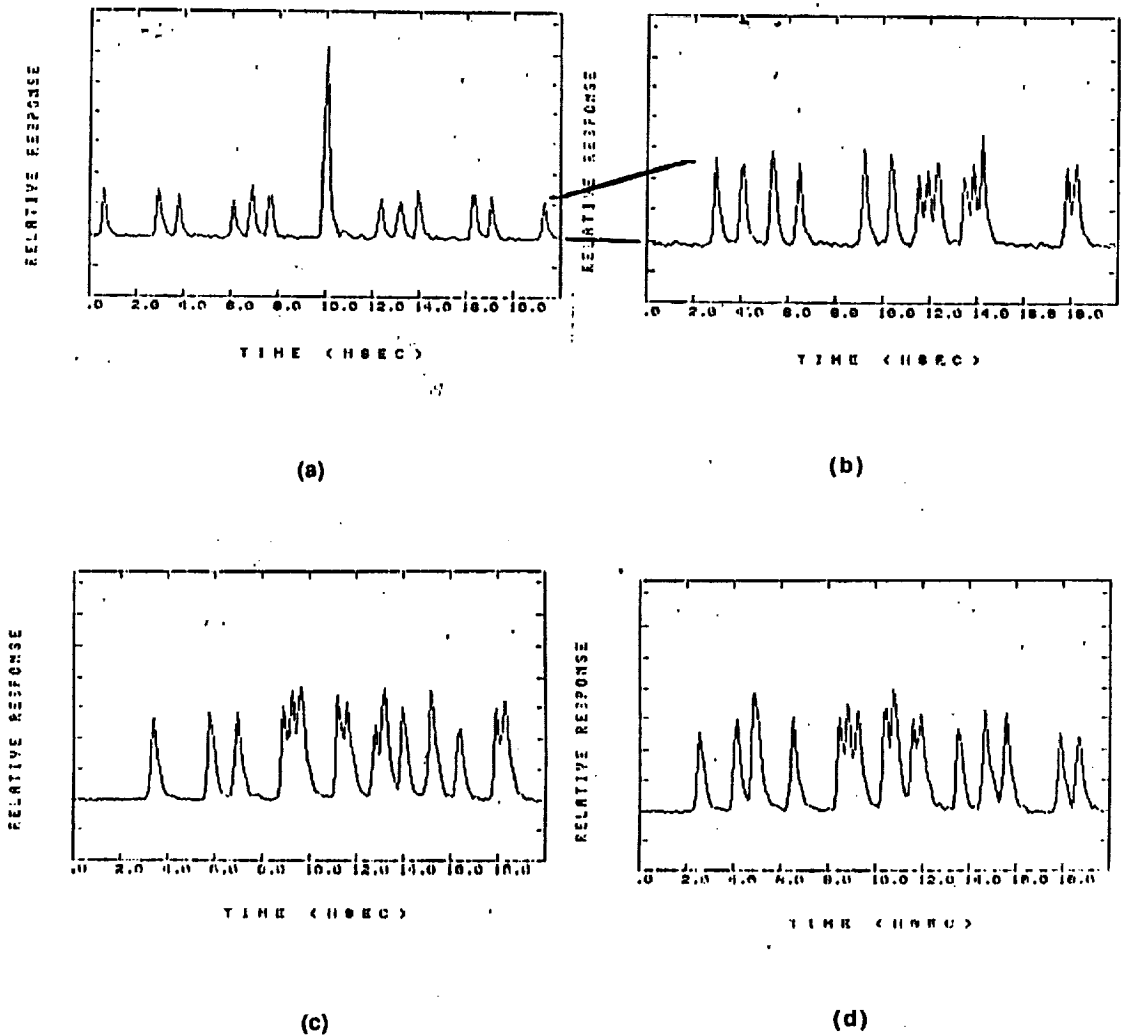
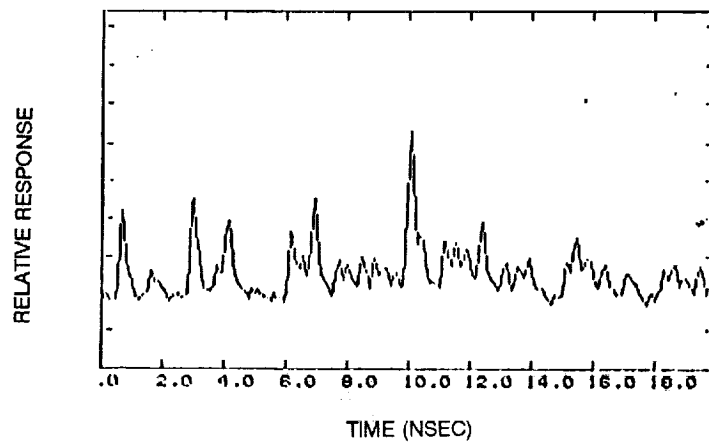
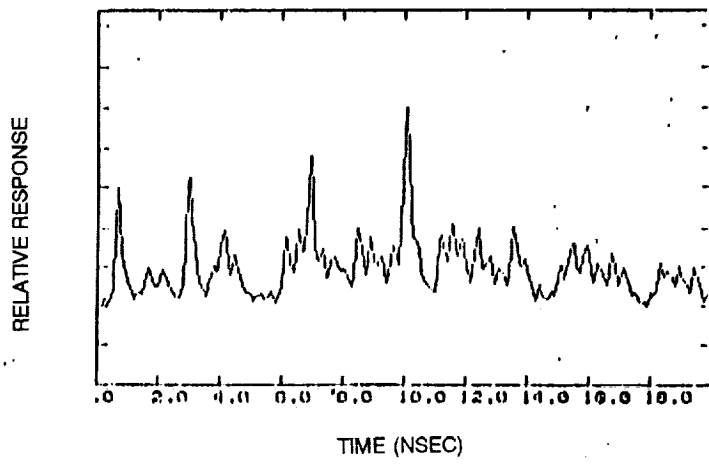


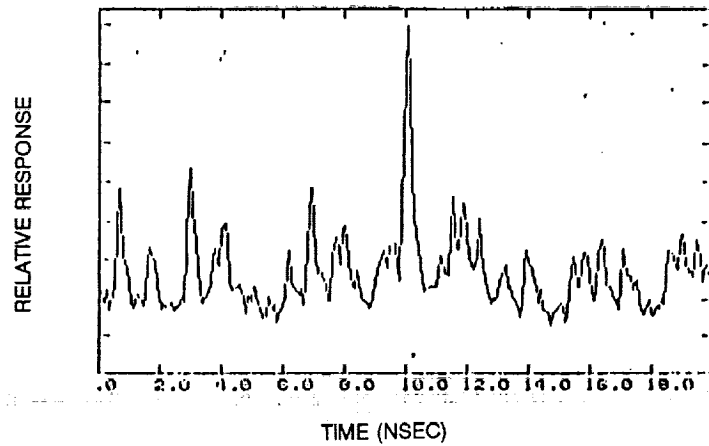
Figure 8-4. Output of User #1's matched decoder for one user transmitting at a time. (a) User #1 transmitting. (b) User #2 transmitting. (c) User #3 transmitting. (d) User #4 transmitting. (a) is the autocorrelation, (b) - (d) are the crosscorrelations. Note scale change.



(c)

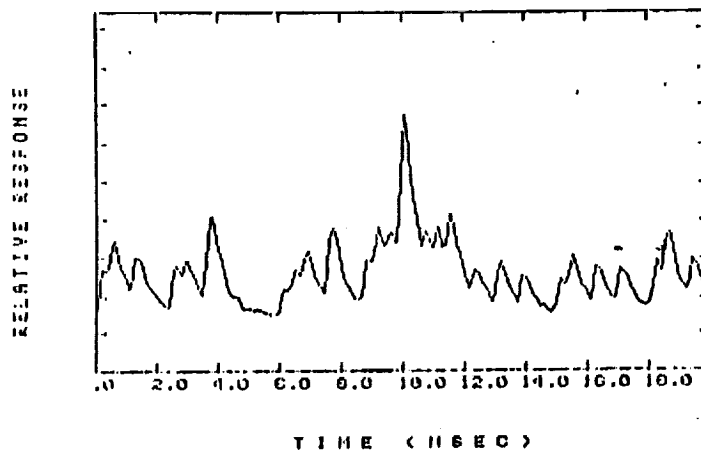


(b)

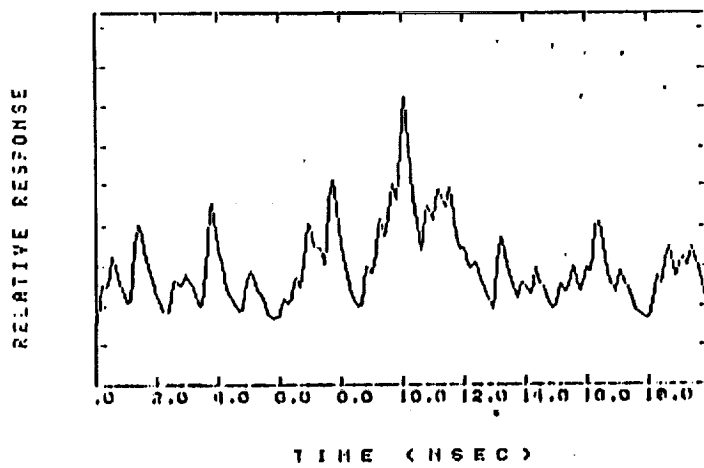


(a)

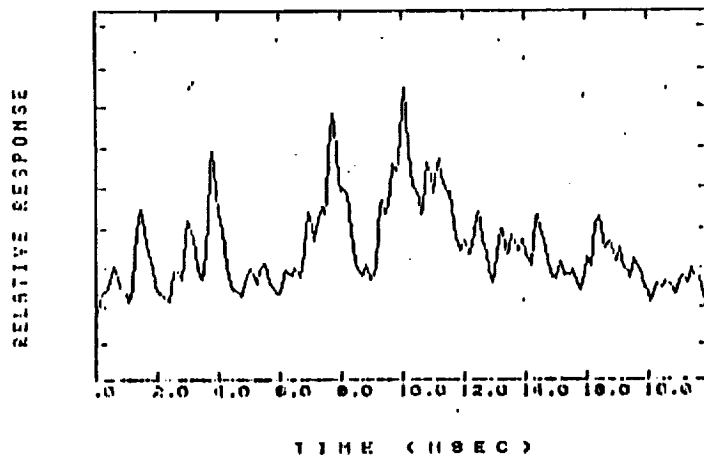
Figure 8-5. Output of User #1's matched decoder for bit-synchronous MUI.
 (a) User #1 and 2 transmitting. (b) User #1, 2, and 3 transmitting.
 (c) User #1, 2, 3, & 4 transmitting. Scale change between (a) and (b).



(a)



(b)



(c)

Figure 8-6. Output of User #1's matched decoder for "worst-case" MUI.
 (a) User #1 and 2 transmitting. (b) User #1, 2, and 3 transmitting.
 (c) User #1, 2, 3, and 4 transmitting.

Temporal/Spatial CDMA

A code set for four users, weight four, and four space channels ($M(4,4,4)$) was implemented. The temporal/spatial (T/S) matrix codes are of the single pulse-per-row (SPR) type. Figure 8-7 shows the breadboard architecture. As in the temporal case, the decoder was chosen to match Encoder #1.

The pulse representation of the matrix codes appear as a pulse on each space channel shifted with respect to one another. Figure 8-8 shows the matrix code assigned to Encoder #1 (User #1), and how the pulses would appear in time and space.

Figure 8-9 shows the decoder output when only one user is transmitting at a time. Notice that unlike the temporal CDMA case, there are no side lobes in the autocorrelation function. Also the crosscorrelation of User #2 and User #4's codes with the decoder are similar. In fact, they are temporally equivalent, but the pulses come from different space channels (indicated). Figure 8-10 shows the decoder output with bit-synchronous MUI. Worst-case MUI has not been performed at this time.

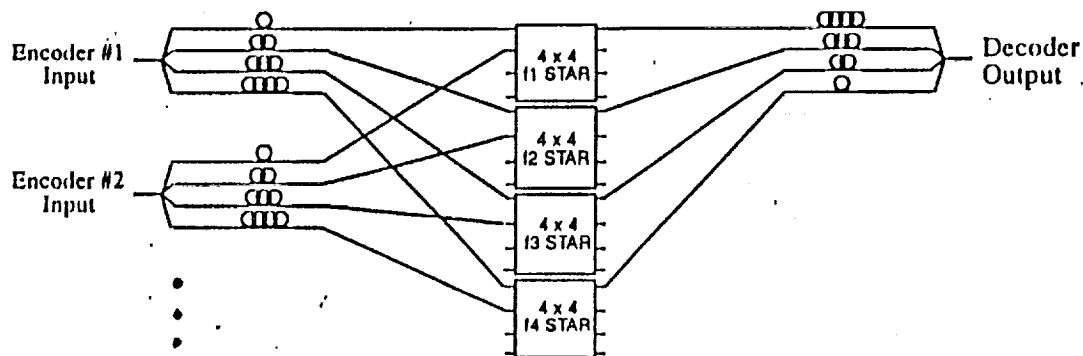


Figure 8-7. Breadboard Architecture for T/S CDMA.

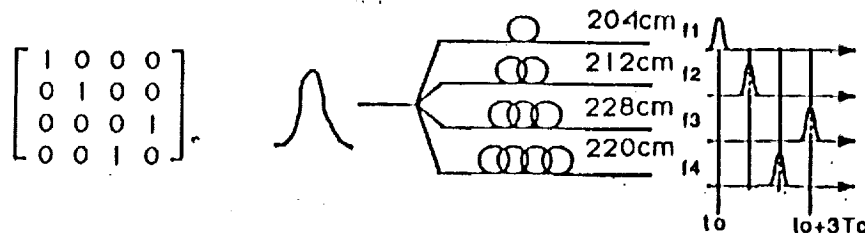


Figure 8-8. User #1's code, encoder, and pulse representation.

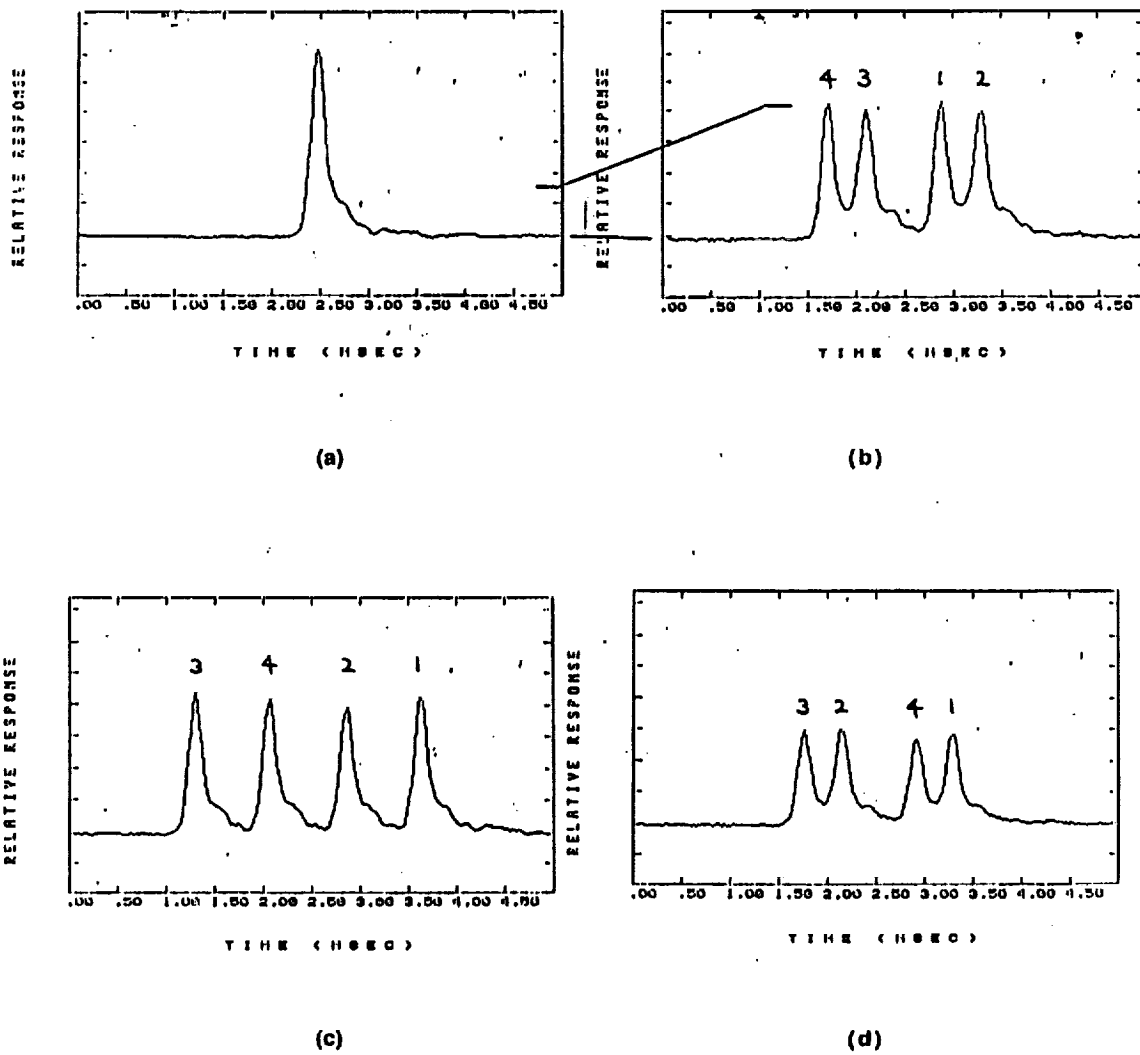
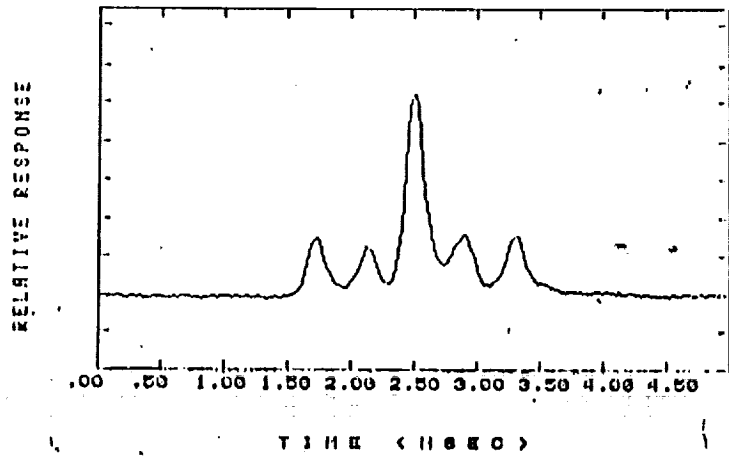
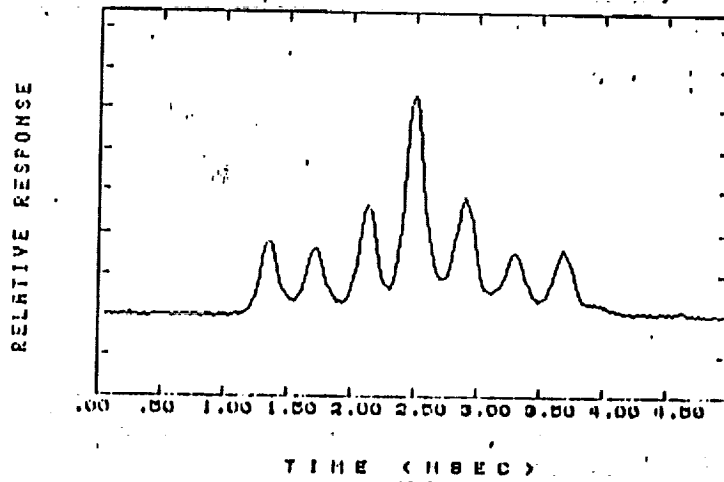


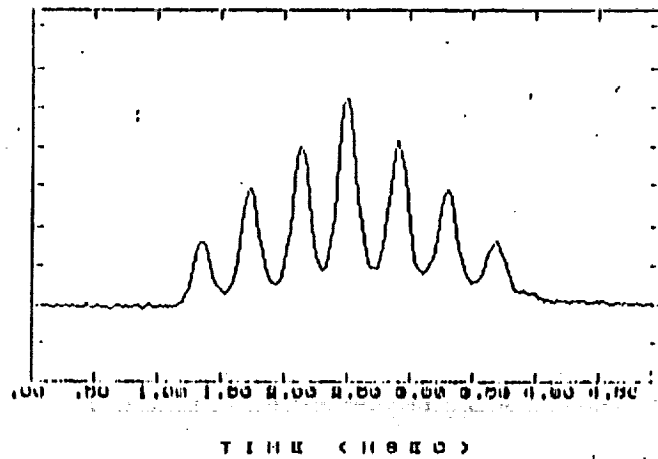
Figure 8-9. Output of User #1's matched decoder for one user transmitting at a time. (a) User #1 transmitting. (b) User #2 transmitting. (c) User #3 transmitting. (d) User #4 transmitting. (a) is the autocorrelation, (b) - (d) are the crosscorrelations. Note scale change. Space channel pulse origin indicated.



(a)



(b)



(c)

Figure 8-10. Output of User #1's matched decoder for bit-synchronous MUI. (a) User #1 and 2 transmitting. (b) User #1, 2, and 3 transmitting. (c) User #1, 2, 3, and 4 transmitting.

9.0 Identification of System/Technology Shortfalls and Future R/R&D Recommendations

We identified the system/technology shortfalls by examining a typical signal flow and identifying actual or potential problem areas. A typical signal flow is depicted in Figure 9-1. The two broken lines are the interfaces between the RF uplink and optical on board router and router and RF downlink, respectively. The signal flow shows all the intervening processes. Blocks or process with a dot identified the actual or potential problem areas discussed below.

Circuit Interface Unit (CIU)

The CIU is not part of the on board router but influences its design and performance. The RF part of the system appears to have multiple parallel channels and multiplexing/demultiplexing. The selected design and its alternate utilize a form of parallel optical transmission. Thus, it is possible that a close examination of the CIU requirements might suggest a more effective interface between the RF and optical signal formats and hardware.

Error Correction Codes (EEC)

The selected design has an estimated raw error rate of about 10^{-3} . If better performance, say, 10^{-9} , is required, error correction codes can be used. In the figure, we show the EEC encoder (ECC/E) operating in the electrical domain and mapping bits into symbols. The ECC/E (and decoder, ECC/D) would have to operate at about 256 Mb/s, which is possible with today's state of the art. Similarly, the laser driver and laser diode then have to operate at 256 Mb/s with pulses of about 0.65 ns. This, too, is possible with communication type semiconductor lasers. But there is limited growth potential in the electrical ECC/laser combination with respect to larger networks and/or higher data rates. This discussion cannot proceed further without (1) a well defined bit error rate requirement and (2) a better understanding (through measurement and analysis) of the real error rate performance of optical matrix CDMA and the associated statistics. Then ECC schemes can be postulated, analyzed, and developed.

Address Command

The address command requires that the sender (encoder) or receiver (decoder) be able to match the CDMA code of the addresses. We have shown in the selection of the preferred candidate that the various addresses are permutations of two basic codes. Thus, the problem here is to define encoders/decoders which physically emulate the permutations of two basic matrix delay line sequences. Trade offs need to be carried out here which compare switching among all possible matrix delays with switching between two sets of delays and then permuting these by means an optical perfect shuffle (such as used in optical computers and neural networks).

Adaptive Threshold

This process/box/function relates to the optical setting of the receiver threshold. The ECC performance is extremely sensitive to this function (see Chapter 7). The threshold is also sensitive to the number of concurrent users and the message rate. Hence, some network and user analysis is required here, together with receiver design and development.

Deskewer

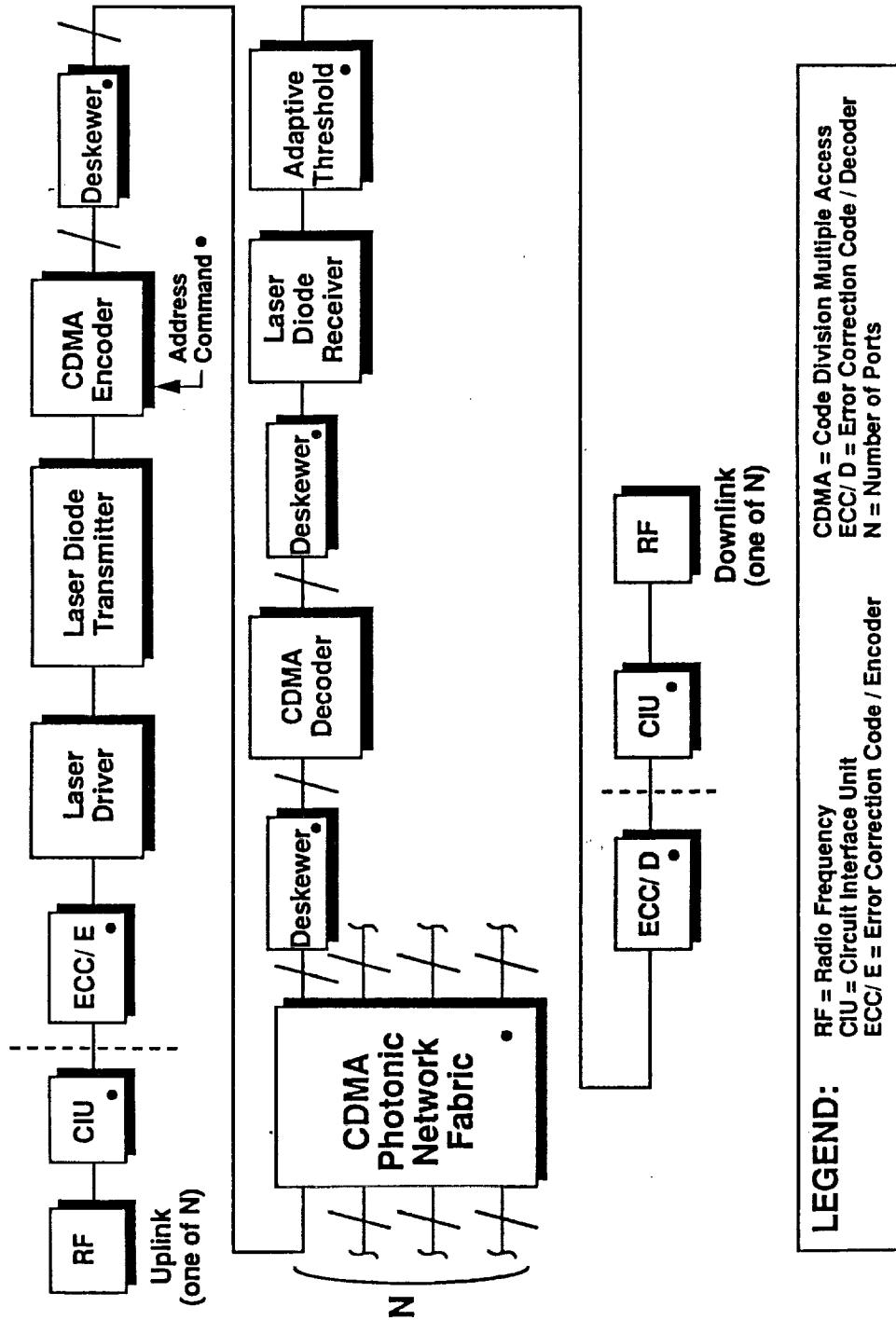
The selected solution is really a parallel optical bus which is sensitive to skew among the parallel channels (fibers). Thus, sources of skew or optical path difference must be sensed and compensated during fabrication and assembly as well as during operation. The "deskewer" is a means of effecting this compensation. It is known how to do this in the lab, but research is required to make this dynamic and fieldable.

CDMA Photonic Network Fabric

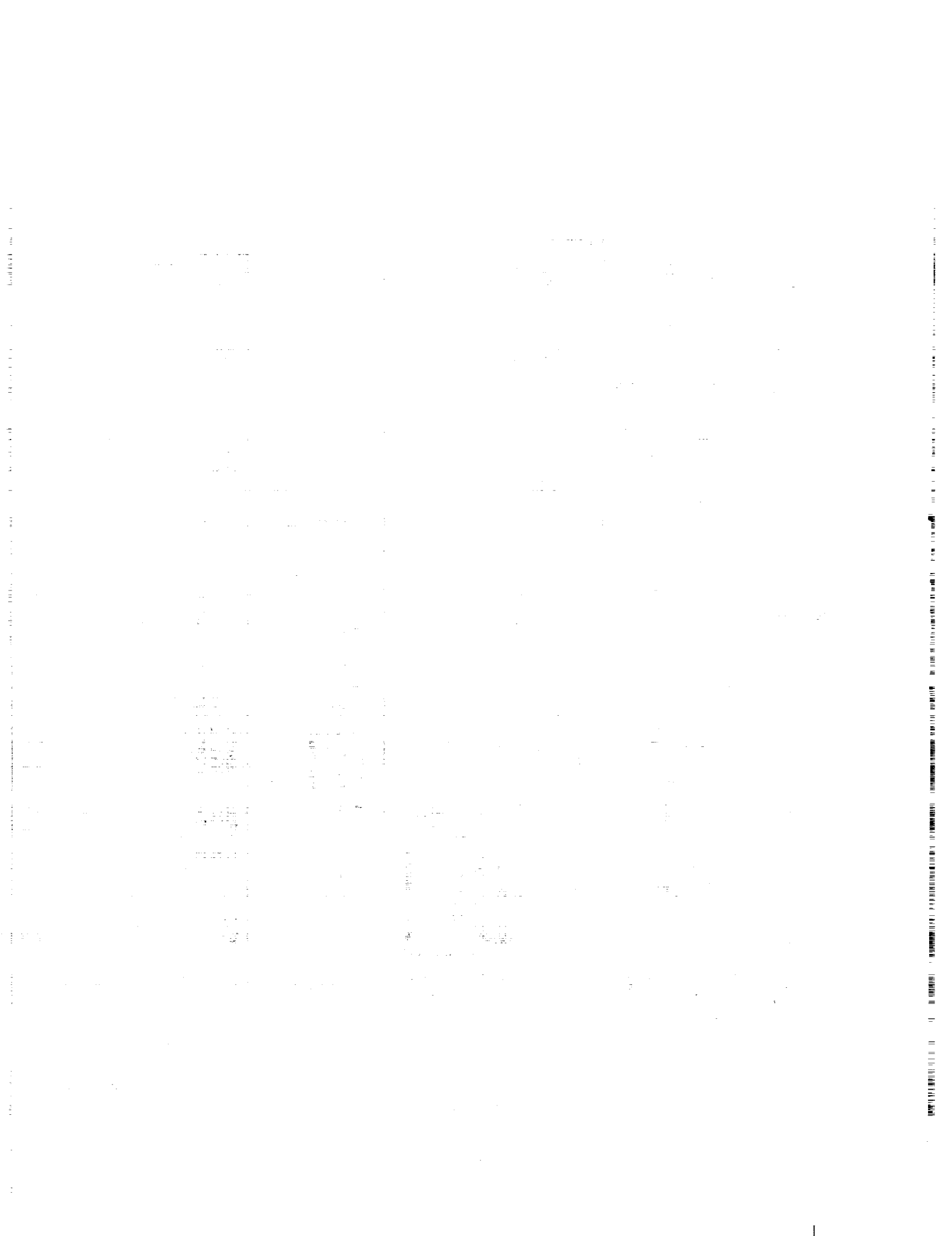
All CDMA network techniques are intrinsically lossy because they incur losses at least as $(1/N)(1/w^2)$, for matrix codes. This leads to the problem of high laser transmitter requirements (~ 10 dBm @ 0.5 ns) or high receiver sensitivity requirements (~ 30 dBm @ 0.5 ns). Many excellent, productized transceivers which otherwise lend themselves to this application are therefore excluded from consideration. These excluded transceivers can become authentic device candidates if the CDMA network had zero loss. The zero loss can be obtained by giving the photonic network fabric gain - for example, by including optical amplifiers in the CDMA network fabric.

Signal Flow in Optical Multiple Access Onboard Router / Switch

Figure 9-1.



06-19-91



10.0 Conclusions and Phase II Recommendations

We have shown by analysis and by design that there exists an optical CDMA solution to the on board routing problem. Such a solution permits 8 concurrent, asynchronous, bursty communications at 180 Mb/s each. The raw error rate would be 10^{-3} , but this could readily be corrected to better than 10^{-9} by incorporating error corrections codes (e.g. LSI Logic has a RS(54,28,8) chip which operates at 320 Mb/s). Alternately, a back-up CDMA design was shown which has extremely good raw error rate performance (10^{-9}), but requires somewhat riskier laser drivers and laser diodes.

In the near term the optical CDMA solution can be implemented with off-the-shelf passive and electro optic components. This implementation would be hardwired and would have to be manually switched by physically changing the encoders or decoders.

The next level of sophistication would switch codes on command from a controller - this could be done by switching delays within an encoder (e.g., using DiCON electro-mechanical matrix switch).

In the far term, we see the encoders, decoders, and network fabric constructed with planar waveguide technology and ribbon cables. Transmitters and receivers, as well as electro optic switches, would be integrated with the planar waveguides. The layered stars themselves would be fabricated as integrated planar structures.

To make the integrated planar technology approach feasible, we need to be able to reduce the laser transmitter power and receiver sensitivity requirements. We need to identify a mechanism for compensating the CDMA losses. Potentially, this mechanism is optical amplification. With optical amplifiers integrated with the networks fabric, the laser power requirements may be reduced to 0 dBm. The many well developed laser transceivers with their associated integrated digital electronics would meet the system requirements.

The above discussion describes a near term/mid term/far term technology roadmap for the optical CDMA switch itself. In parallel, effort is also required in various system areas. For example, the interface between the RF and the optical systems at both ends of the on board router needs to be better defined. It may well be that some aspects of the optical CDMA depend on trade offs on the RF side of the interface.

A near term version of the optical CDMA should be used to measure the real raw error rate and its statistics. Then error correction code research should be performed on these data. Special effort should be spent on the problems which will arise in the inevitable transition to more users and higher data rates - when current ECC chip technology is no longer applicable. Then we must find optical solutions.

We found, in working with the subscale CDMA breadboard that special alignment and test procedures had to be developed. Besides having to balance the optical paths of the encoders and decoders, the optical power in each channel had to be balanced so that the receiver could correctly pick out the signal from the clutter. In the future, these procedures need to be incorporated into the design of the optical CDMA switch. This would permit the system to quickly calibrate and adjust itself during the initialization or self test routine.

Because the optical CDMA approached based on temporal/spatial matrices is so flexible and so readily meets the on board routing requirements, we recommend additional R/R&D in six areas:

1. Further development of matrix codes especially T/S-SPR combinations
2. Reconfigurable matrix encoders or decoders
3. Zero loss CDMA photonic networks (this would allow a larger selection of communications transceivers, more users, or higher data rates)
4. Criteria and techniques for establishing receiver thresholds in dynamic, asynchronous multi user environments
5. Error correction codes applicable to optical multiple access networks operating at greater than 200 Mb/s
6. System checkout, calibration, and alignment procedures.

Most of the above recommendations can be carried out by developing and characterizing the complete 8 user, 180 Mb/s matrix CDMA on board router described in this report.

11.0 References

- [1] H. S. Hinton, "Photonic time-division switching systems," IEEE Circuits and Devices Mag., vol. 5, pp. 39-43, 1989.
- [2] A.J. Mendez, "Fiber optic communication networks based on Code Division Multiple Access (CDMA) Techniques," paper presented to the IEEE / Santa Monica Section, March 20, 1991.
- [3] A. J. Mendez, S. Kuroda, R. Gagliardi, and E. Garmire, "Generalized temporal code division multiple access (CDMA) for optical communications," SPIE Proc., vol. 1175, pp.208-217, 1989.
- [4] F. Khansefid, "Sets of (0,1) sequences with application to optical fiber networks," USCEE Report CSI-88-02, August, 1988.
- [5] J.A. Salehi, A.M. Weiner, and J.P. Heritage, "Coherent ultrashort light pulse code division multiple access communication systems," Jr Ltw Tech, Vol 8, p 428 (1990).
- [6] R. M. Gagliardi, A. J. Mendez, "Pulse combining and time-space coding for multiple access with fiber arrays," Summer Topical Meeting on Optical Multiple Access Networks, paper OMth14, Monterey, CA, July 1990.
- [7] A.J. Mendez, E. Park, R.M. Gagliardi, H. Taylor, and E. Garmire "Analysis of multi user interference in three classes of optical multiple access codes," 1990 IEEE/LEOS Summer Topical Meeting on Optical Multiple Access Networks, paper PD5, Monterey, CA, July 1990.
- [8] S. W. Golomb, and H. Taylor, "Two dimensional synchronization patterns for minimum ambiguity," IEEE Trans on Info Theory, Vol IT-28, p 600 (1982).
- [9] L.D. Tzeng, R.E. Frahun, and W. Asous, " A high performance receiver for 622 Mb/s direct detection systems," IEEE Photon Tech Letters, Vol 2, p 179 (1990)
- [10] M. Stern, J. P. Heritage, R. N. Thurston, and S. Tu, "Self-phase modulation and dispersion in high data rate fiber-optic transmission systems," J. Lightwave Technol., vol. 8, no. 7, pp. 1009-1016.
- [11] M. Tur, A. Arie, "Phase induced intensity noise in concatenated fiber-optic delay lines," J. Lightwave Technol., vol. 6, no. 1, pp. 120-130.

REPORT DOCUMENTATION PAGE

Form Approved
OMB No. 0704-0188

Public reporting burden for this collection of information is estimated to average 1 hour per response, including the time for reviewing instructions, searching existing data sources, gathering and maintaining the data needed, and completing and reviewing the collection of information. Send comments regarding this burden estimate or any other aspect of this collection of information, including suggestions for reducing this burden, to Washington Headquarters Services, Directorate for Information Operations and Reports, 1215 Jefferson Davis Highway, Suite 1204, Arlington, VA 22202-4302, and to the Office of Management and Budget, Paperwork Reduction Project (0704-0188), Washington, DC 20503.

1. AGENCY USE ONLY (Leave blank)	2. REPORT DATE March 1992	3. REPORT TYPE AND DATES COVERED Final Contractor Report	
4. TITLE AND SUBTITLE Optical Multiple Access Techniques for On-Board Routing		5. FUNDING NUMBERS WU-321-01 C-NAS3-25925	
6. AUTHOR(S) Antonio J. Mendez, Eugene Park, and Robert M. Gagliardi		7. PERFORMING ORGANIZATION NAME(S) AND ADDRESS(ES) Mendez R&D Associates P.O. Box 2756 El Segundo, California 90245	
8. PERFORMING ORGANIZATION REPORT NUMBER None		9. SPONSORING/MONITORING AGENCY NAMES(S) AND ADDRESS(ES) National Aeronautics and Space Administration Lewis Research Center Cleveland, Ohio 44135-3191	
10. SPONSORING/MONITORING AGENCY REPORT NUMBER NASA CR-187221		11. SUPPLEMENTARY NOTES Project Manager, William D. Ivancic, Space Electronics Division, NASA Lewis Research Center, (216) 433-3494.	
12a. DISTRIBUTION/AVAILABILITY STATEMENT Unclassified - Unlimited Subject Category 32		12b. DISTRIBUTION CODE	
13. ABSTRACT (Maximum 200 words) The purpose of this research contract was to design and analyze an optical multiple access system, based on Code Division Multiple Access (CDMA) techniques, for on board routing applications on a future communication satellite. The optical multiple access system was to effect the functions of a circuit switch under the control of an autonomous network controller and to serve eight (8) concurrent users at a point to point (port to port) data rate of 180 Mb/s. (At the start of this program the bit error rate requirement (BER) was undefined, so it was treated as a design variable during the contract effort.) CDMA was selected over other multiple access techniques because it lends itself to bursty, asynchronous, concurrent communication and potentially can be implemented with off the shelf, reliable optical transceivers compatible with long term unattended operations. Temporal, temporal/spatial hybrids and single pulse per row (SPR, sometimes termed "sonar matrices") matrix types of CDMA designs were considered. The design, analysis, and trade offs required by the statement of work selected a temporal/spatial CDMA scheme which has SPR properties as the preferred solution. This selected design can be implemented for feasibility demonstration with off the shelf components (which are identified in the bill of materials of the contract Final Report). The photonic network architecture of the selected design is based on M(8,4,4) matrix codes. The network requires eight multimode laser transmitters with laser pulses of 0.93 ns operating at 180 Mb/s and 8-13 dBm peak power, and 8 PIN diode receivers with sensitivity of -27 dBm for the 0.93 ns pulses. The wavelength is not critical but 830 nm technology readily meets the requirements. The passive optical components of the photonic network are all multimode and off the shelf. Bit error rate (BER) computations, based on both electronic noise and intercode crosstalk, predict a raw BER of (10 ⁻³) when all eight users are communicating concurrently. If better BER performance is required, then error correction codes (ECC) using near term electronic technology can be used. For example, the M(8,4,4) optical code together with Reed-Solomon (54,38,8) encoding provides a BER of better than (10 ⁻¹¹). The optical transceiver must then operate at 256 Mb/s with pulses of 0.65 ns because the "bits" are now channel symbols. A subscale CDMA network which was built with resources outside of this contract was used to demonstrate and evaluate the concepts developed in this program. The test results support and validate the analysis and claims made for the preferred solution. Potential future applications of the kind of optical CDMA network described in the contract include (1) communication satellite on board circuit switch, (2) optical backplane busses for parallel processing computers, (3) optical local area networks with simple protocols, (4) networking of embedded sensors (as in smart skins and smart structures, (5) digital display generators serving multiple, multipurpose displays, and (6) optical backplane busses for avionics racks in aircraft designed for integrated modular avionics.			
14. SUBJECT TERMS On-board routing; Optical multiple access; Code division multiple access		15. NUMBER OF PAGES 56	16. PRICE CODE A04
17. SECURITY CLASSIFICATION OF REPORT Unclassified	18. SECURITY CLASSIFICATION OF THIS PAGE Unclassified	19. SECURITY CLASSIFICATION OF ABSTRACT Unclassified	20. LIMITATION OF ABSTRACT